Groundwater residence time and aquifer recharge in multilayered, semi-confined and faulted aquifer systems using environmental tracers

Article *in* Journal of Hydrology · March 2017

DOI: 10.1016/jjhydrol.2016.12.036

CITATIONS
3

READS
399

6 authors, including:

Jordi Batlle-Aguilar

76 PUBLICATIONS **639** CITATIONS

SEE PROFILE

Eddie Banks

Flinders University

47 PUBLICATIONS **351** CITATIONS

SEE PROFILE

Okke Batelaan

Flinders University

352 PUBLICATIONS **5,659** CITATIONS

SEE PROFILE

Matthias Brennwald

Eawag, Swiss Federal Institute of Aquatic Science and Technology ||| Gasometrix …

152 PUBLICATIONS **1,304** CITATIONS

SEE PROFILE

Journal of Hydrology 546 (2017) 150–165

Contents lists available at ScienceDirect

Journal of Hydrology

journal homepage: www.elsevier.com/locate/jhydrol

Research papers

Groundwater residence time and aquifer recharge in multilayered, semi-confined and faulted aquifer systems using environmental tracers

Jordi Batlle-Aguilar [a,*], Eddie W. Banks [b], Okke Batelaan [b], Rolf Kipfer [c,d], Matthias S. Brennwald [c], Peter G. Cook [b]

[a] Kansas Geological Survey, University of Kansas, 1930 Constant Avenue, Lawrence, KS 66047, USA
[b] National Centre for Groundwater Research and Training (NCGRT), School of the Environment, Flinders University, GPO Box 2100, Adelaide, SA 5001, Australia
[c] Department of Water Resources and Drinking Water, Eawag: Swiss Federal Institute of Aquatic Science and Technology, Ueberlandstrasse 133, CH-8600 Dübendorf, Switzerland
[d] Institute of Geochemistry and Petrology, ETH Zurich, CH-8092 Zurich, Switzerland

ARTICLE INFO

Article history:
Received 18 July 2016
Received in revised form 18 October 2016
Accepted 21 December 2016
Available online 24 December 2016
This manuscript was handled by L. Charlet, Editor-in-Chief, with the assistance of Federico Maggi, Associate Editor

Keywords:
Groundwater mixing
Flow velocity
Helium-4
Radiocarbon

ABSTRACT

The potential of environmental tracers ($\delta^{18}O$, $\delta^{2}H$, $\delta^{13}C$, ^{14}C, ^{4}He, ^{20}Ne, ^{40}Ar, N_2) to assist our understanding of recharge processes, groundwater flow velocities and residence times in semi-confined, multilayered and faulted aquifer systems was tested in a coastal system with Quaternary sediments overlying Tertiary aquifers and fractured bedrock. Carbon-14 groundwater ages were found to increase with depth and distance (<1000 y near the recharge area to >30,000 y near the coast), confirming that the system is semi-confined and the palaeometeoric origin of groundwater as suggested by water stable isotopes. The presence of old groundwater near the top of deep semi-confined aquifers suggests that recharge mainly occurs in the ranges east of the basin. This is also supported by Cl concentrations, which are higher in the overlying Quaternary aquifers. Groundwater flow velocities between 0.3 and 1.8 m y^{-1} were estimated using ^{14}C ages, resulting in basin recharge estimates between 0.3×10^{7} and 2×10^{7} m^3 y^{-1}. Radiocarbon and ^{4}He-estimated flow velocities were generally in good agreement, although ^{4}He accumulation rates ranging between 8×10^{-12} and 1×10^{-10} cm^3 STP g^{-1} y^{-1} and $1.7–7.1 \times 10^{-7}$ cm^3 STP g^{-1} km^{-1} confirmed slower flow velocities in some areas. These areas could not be captured using ^{14}C. Faults were found to play a paramount role on mixing old fluids rich in salts and ^{4}He, although it was not possible to demonstrate the role of faults in changing flow velocities, this requiring a higher density of sampling points. Our study shows that environmental tracers have potential to study flow processes in semi-confined, faulted, multilayered aquifer systems, provided a high density of sampling points is available.

1. Introduction

Population growth and rising water demands for industrial, agricultural, recreation and household uses, combined with ongoing climate change (e.g., extreme events), is driving many regions into an imbalance of supply and demand (Vairavamoorthy et al., 2008). Millions of people around the world depend on groundwater, particularly in semi-arid and arid environments (e.g., Mays, 2013). Water management practices in these environments require a thorough and robust scientific understanding of recharge processes, residence time of groundwater and renewability of the resource (Mahlknecht et al., 2004). Determination of groundwater flow paths and residence times is critical for the sustainable management and exploitation of any aquifer, but quantification of these processes is often challenged by complex hydrogeological systems, especially in multilayered and faulted aquifers.

Environmental tracers have been widely used for determining the sources of groundwater and residence times (Cook and Bohlke, 2000). Among them, the most extensively used for estimating residence times of slow moving groundwater systems are radiocarbon (^{14}C) and helium-4 (^{4}He). Groundwater apparent age determination with radiocarbon is based on radioactive decay (half-life of 5730 years; Clark and Fritz, 1997) from an initial ^{14}C activity which is usually assumed to be constant (Kalin, 2000). However, ^{14}C can be strongly affected by rock-water interactions (Clark and Fritz, 1997). For example, dissolution of calcite or dolomite can result in the addition of very old ^{14}C, diluting the ^{14}C

* Corresponding author.
E-mail addresses: jba@kgs.ku.edu (J. Batlle-Aguilar), eddie.banks@flinders.edu.au (E.W. Banks), okke.batelaan@flinders.edu.au (O. Batelaan), rolf.kipfer@eawag.ch, rkipfer@ethz.ch (R. Kipfer), matthias.brennwald@eawag.ch (M.S. Brennwald), peter.cook@flinders.edu.au (P.G. Cook).

http://dx.doi.org/10.1016/j.jhydrol.2016.12.036
0022-1694/

Nomenclature

AF	Alma Fault
AMS	Accelerator Mass Spectrometry
asl	Above sea level
BPF	Blanche Point Formation (aquitard)
DEWNR	Department of Environment, Water and Natural Resources
DO	Dissolved Oxygen
EBF	Eden-Burnside Fault
FRA	Fractured (aquifer)
GE-MIMS	Gas-Equilibrium Membrane-Inlet Mass Spectrometer
HVF	Hope Valley Fault
K_H	Horizontal hydraulic conductivity
K_V	Vertical hydraulic conductivity
LMWL	Local Meteoric Water Line
mbg	Meters below ground
mbwt	Meters below water table
MLR	Mount Lofty Ranges
MP	Munno-Para (aquitard)
n	Number of samples
n_e	Porosity
PDB	Pee Dee Belemnite
PF	Para Fault
pmC	percent of modern Carbon
ppm	Parts per million
PWF	Para West Fault
Q	Quaternary (aquifer)
SEC	Specific Electrical Conductivity
SMOW	Standard Mean Ocean Water
STP	Standard conditions for Temperature and Pressure (273.15 K and 1 bar)
TDIC	Total Dissolved Inorganic Carbon
TDS	Total Dissolved Solids
TOC	Top Of Casing
T1–T4	Tertiary (aquifers)

activity of atmospheric CO_2 at recharge and causing an overestimation of groundwater ages. Helium-4 accumulates over time due to subsurface production by radioactive decay of Uranium (U) and Thorium (Th) within the aquifer matrix (Andrews and Lee, 1979; Solomon, 2000) and external fluxes from the mantle (Torgersen and Clarke, 1985; Torgersen and Ivey, 1985). Groundwater age determination with ^{4}He depends upon knowledge of the ^{4}He accumulation rate, which is usually obtained by comparison with ^{14}C (Kulongoski et al., 2003; Torgersen and Clarke, 1985; Wei et al., 2015) or ^{3}H/^{3}He ages (Beyerle et al., 1999), or from measurements of production rates on aquifer materials (Lehmann et al., 2003; Mayer et al., 2014).

Many studies that have used environmental tracers to determine groundwater residence time and recharge processes were carried out in unconsolidated and unconfined aquifers (Cartwright and Morgenstern, 2012; Houben et al., 2014; McMahon et al., 2004), or multilayered sedimentary aquifers free of major faults (Castro, 2004; Plummer et al., 2012; Price et al., 2003). Tracers have also been used in more complex, fractured aquifers, to qualitatively identify the origin of groundwater (Roques et al., 2014), the role of faults in mixing deep old groundwater and highly saline endogenic fluids (e.g., Kaudse et al., 2016; Raiber et al., 2015; Williams et al., 2013) and to constrain fracture and matrix diffusion parameters (Cook et al., 2005; Cook and Simmons, 2013) and groundwater recharge rates (Cook et al., 2005; Cook and Robinson, 2002). However, quantitative studies to understand regional flow systems in complex, fractured and faulted environments are rare (Doyle et al., 2015; Manning and Solomon, 2005).

Faults in hydrogeological systems can act as preferential flow pathways but also flow barriers, and in either case they may have an important influence on groundwater flow (Castro and Goblet, 2005). High hydraulic gradients across faults may indicate that these structures act as horizontal flow barriers (Bense et al., 2008; Mayer et al., 2007), although the use of chemical tracers (Stoessell and Prochaska, 2005), temperature (Bense et al., 2008), numerical models (Bense and Person, 2006) and pumping tests (Medeiros et al., 2010) may provide evidence for cross-fault flow. Recently Bense et al. (2013) recognized that environmental tracers can be a promising tool to provide additional insights on the role of faults in hydrogeological systems. However, to our knowledge, there have not been any studies that have examined the role of faults on groundwater age distributions in regional aquifers, or the potential for environmental tracers to provide information on the role of faults in groundwater flow systems.

In this paper, we examine the potential of environmental tracers to assist our understanding on groundwater flow and recharge processes, and to determine groundwater flow velocities and residence time in complex faulted and multilayered hydrologic systems. Major ions, isotopic tracers (δ^2H, δ^{18}O, δ^{13}C, ^{14}C) and dissolved gases (^{4}He, ^{20}Ne, ^{40}Ar, N_2) were analyzed on groundwater sampled from 54 wells in the Adelaide Plains groundwater system (South Australia). The multilayered Adelaide Plains groundwater system is separated from bedrock uplands by fault systems, and also dissected by a number of other major faults causing significant vertical displacement of aquifers.

2. Study area

The Adelaide Plains region of South Australia covers approximately 1100 km^2, and is bounded by the Gulf St. Vincent in the west, the Western Mount Lofty Ranges (MLR) in the east, the Eden-Burnside Fault (EBF) in the south and the Gawler River in the north (Fig. 1). The surface elevation ranges from sea level at the coast to a maximum of 727 m above sea level (a.s.l.) in the Western MLR. The area has a Mediterranean dry climate, with mean annual rainfall of 400 mm in the Plains (2005–2014; Australian Government, Bureau of Meteorology, Adelaide Airport station number 023034; elevation 2 m a.s.l.) and 1040 mm in the MLR (2005–2014; Australian Government, Bureau of Meteorology, Uraidla station number 023750; elevation 487 m a.s.l.). The majority of rainfall occurs during the winter months (late May to August) with as little as 15% of the annual rainfall falling during the summer months (December–March).

Two main rivers, the Gawler River and the River Torrens, drain westerly from the Western MLR towards the Gulf St. Vincent. Their mean annual flow discharge (2010–2015) are 0.5 m^3 s^{-1} (gauge ID A5050510) and 0.9 m^3 s^{-1} (gauge ID A5040529), respectively (http://wds.amlr.waterdata.com.au/Amlr.aspx). Despite being perennial rivers, their flow dramatically decreases during summer, and may cease during extended dry periods. There are also several ephemeral creeks that flow from the Western MLR and discharge either into the Gawler and Torrens rivers, or directly into the Gulf St. Vincent. Their flow varies considerably both seasonally and

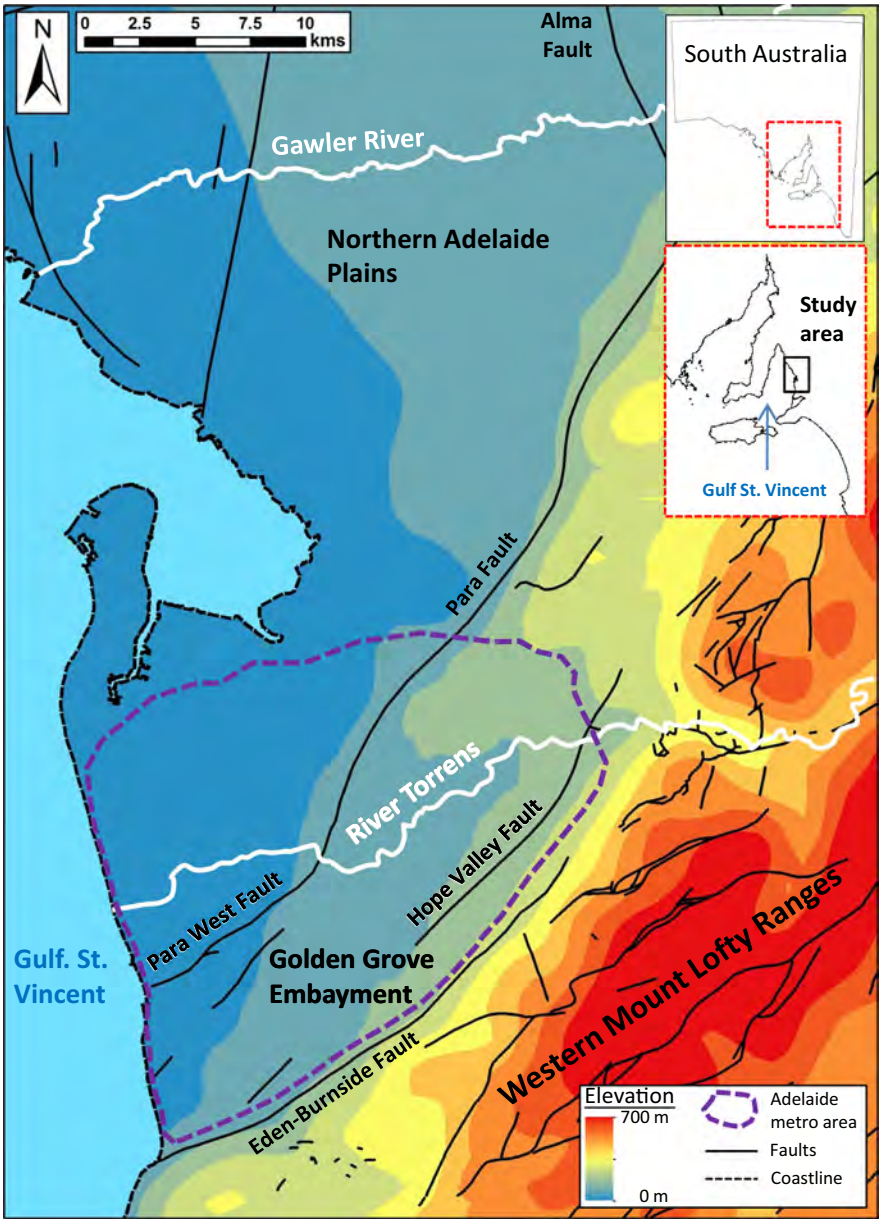

Fig. 1. The Adelaide Plains study area. Major faults, shown with solid black lines, define the topography of the Adelaide Plains, with contrasting hydraulic gradients between the Plains and the Western MLR. The metropolitan area of Adelaide is shown with purple dashed line.

annually, and their mean annual flow discharge is around 0.05 $m^3 s^{-1}$ (e.g. gauge ID A5040901 at Brownhill Creek), mostly occurring during autumn and winter.

Water supply for the metropolitan area of Adelaide is primarily sourced from the Murray River (75 km south east of Adelaide) and a number of reservoirs within the Western MLR. The water supply has been recently complemented with a desalination plant that draws water from the Gulf St. Vincent to meet increasing demands and secure water supply during prolonged droughts.

The region can be subdivided into the Northern and Central Adelaide Plains and the Golden Grove Embayment (or Southern Plains; Fig. 1). The Northern Adelaide Plains is an important agricultural area with intensive irrigation, contrasting with the urbanized areas of Central and Southern Adelaide Plains (including the metropolitan areas of the city of Adelaide), where groundwater is mostly used for recreational and industrial activities (Harrington and Cook, 2014). Many wells in the Northern Adelaide Plains were artesian before intensive agriculture started in the 1940s (Baird, 2010), and groundwater was flowing towards the coast, perpendicular to the coast line (Fig. S1). By 1960, artesian conditions were lost and cones of depression of up to 60 m drawdown were formed. Groundwater levels in the Northern Adelaide Plains have remained relatively constant in the last 20 y, while important cones of depression appeared during the last two decades in the Central Adelaide Plains as a result of industrial activities (DFW, 2011; Georgiou et al., 2011) (Fig. 2). The forecast increase in groundwater demand due to population growth in this already stressed system, raises questions about the sustainability of groundwater quantity and quality.

3. Geological and hydrogeological setting

The Adelaide Plains is part of the sedimentary St. Vincent Basin, and consists of sub-horizontal Tertiary (Cenozoic) sediments bounded below and to the east by fractured Proterozoic rocks,

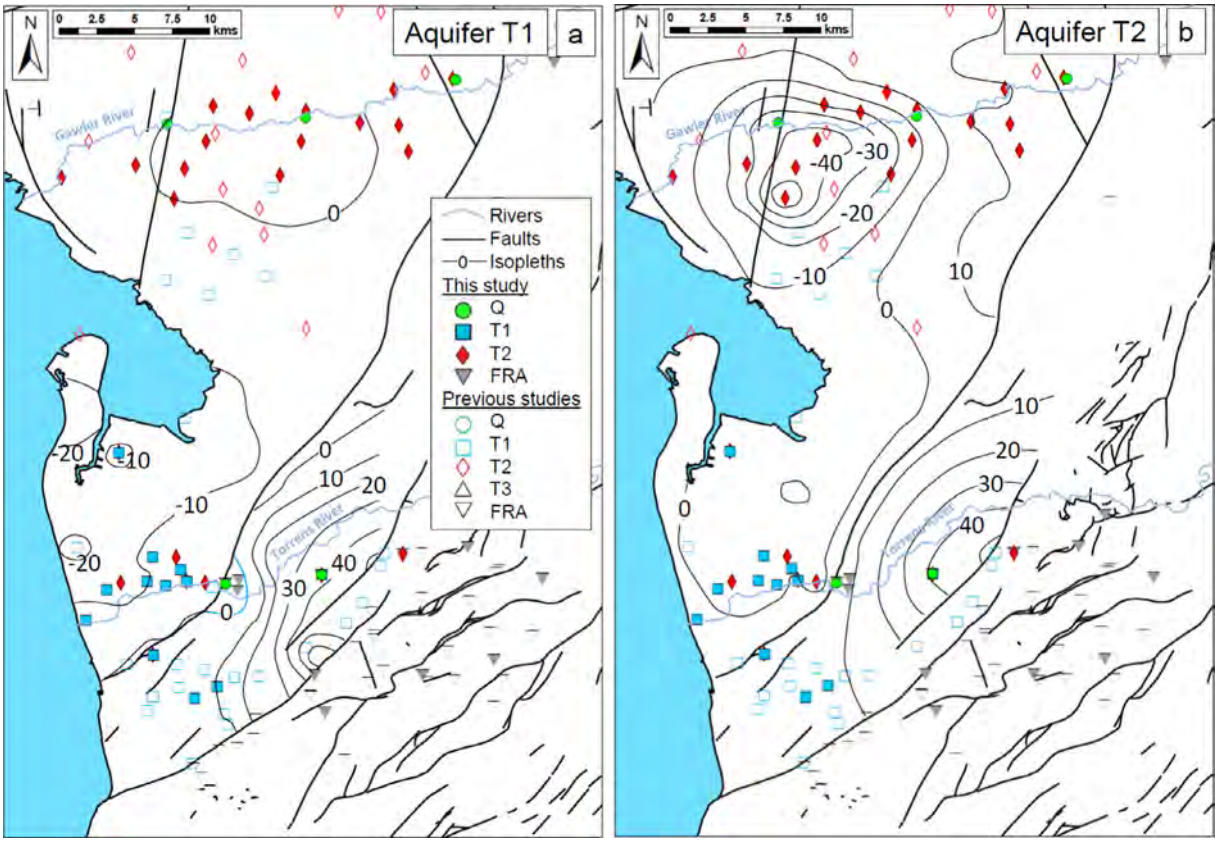

Fig. 2. Piezometric maps of (a) aquifer T1 and (b) aquifer T2 for 2013–2014. It is noticeable the important cone of depression in the Northern Adelaide Plains (T2 aquifer) and other minor cones in the Central Plains (T1 aquifer) west of the Para Fault (PF).

and to the west by the Gulf St. Vincent. Two major fault zones – the EBF which bounds the study area to the south and east, and the Para Fault (PF), which is located in the northern and central portion of the study area (Fig. 1), define the hydrostratigraphy and topography of the Adelaide Plains (Gerges, 1999; Zulfic et al., 2008a; Zulfic et al., 2008b). The PF is a major geological boundary delineating the deposits into two main sub-basins; the Central Adelaide Plains and the Golden Grove Embayment. There is much greater thickness of sediments to the west of the PF (up to ~600 m thickness compared to <150 m east of the PF).

The geology defines a multilayered aquifer system made up of Tertiary and Quaternary sediments (Fig. 3). The Quaternary (Q) sediments are generally subdivided into six aquifers (designated Q1 to Q6), semi-confined by low permeability layers. Horizontal hydraulic conductivity (K_H) of the Q aquifers has been estimated to be between 1×10^{-5} m s^{-1} and 1×10^{-4} m s^{-1}. The vertical hydraulic conductivity (K_V) of semi-confining layers in the Q aquifer is highly variable in space, from 5.8×10^{-12} m s^{-1} to 7×10^{-9} - m s^{-1}. In the Tertiary sediments (sandstone and limestone), four different aquifers are distinguished (T1 to T4). The T1 aquifer, with horizontal hydraulic conductivity between 2 and 5×10^{-5} m s^{-1} sits below the Q6, and is bounded at the bottom by the Munno-Para (MP) clay aquitard, which K_V ranges between 10^{-12} m s^{-1} and 10^{-10} m s^{-1}, with porosity (n_e) between 0.4 and 0.65. The T2 aquifer is bounded at the top by the MP aquitard and the bottom by the Blanche Point Formation (BPF). Hydraulic conductivity of the T2 aquifer has been estimated to be between 7.6×10^{-6} m s^{-1} and 3.1×10^{-5} m s^{-1}, and n_e ranging between 0.37 and 0.45 (Baird, 2010; Gerges, 1999). The much deeper T3 and T4 aquifers have a variable thickness between 5 and 60 m in the Adelaide Plains, and are underlain by the fractured bedrock (FRA) aquifer.

In the Northern Adelaide Plains the T1 aquifer is discontinuous and water for irrigation is primarily extracted from the T2 aquifer. Both the T1 and the T2 aquifers are heavily exploited for industrial use in the Central Adelaide Plains. The T1 aquifer is also discontinuous in the eastern parts of the Golden Grove Embayment. There, the Quaternary aquifers often sit on top of the T2 aquifer, and are primarily exploited for domestic water use. Water from the Quaternary and FRA aquifers in the MLR is used for domestic water supply and irrigation of agricultural and horticultural crops. The two deeper Tertiary aquifers (T3 and T4) are not extensively used due to the cost of drilling to their depths (up to 500 m) and their high salinity (up to 100,000 mg L^{-1}) (Gerges, 1999). In general, groundwater extraction is far more prevalent from the T1 and T2 aquifers west of the PF.

The current conceptual model of the Adelaide Plains groundwater system is that water in the Tertiary aquifers (T1 and T2) is mainly recharged in the MLR, where rainfall infiltrates into the FRA aquifer and flows west across the faults into the Tertiary aquifers to finally discharge into Gulf St.Vincent (Georgiou et al., 2011; Gerges, 1999). Rainfall is also believed to recharge the Quaternary aquifer, although vertical leakage into the T1 and T2 aquifers, despite uncertain, is believed to be low due to the presence of horizontal semi-confining layers in the Quaternary system.

4. Materials and methods

4.1. Drilling design and groundwater sampling

Six well nests (IDs 1, 3, 5, 6 and 12) were drilled to complement the existing network of monitoring wells in the Adelaide Plains that are maintained by the Department of Environment, Water

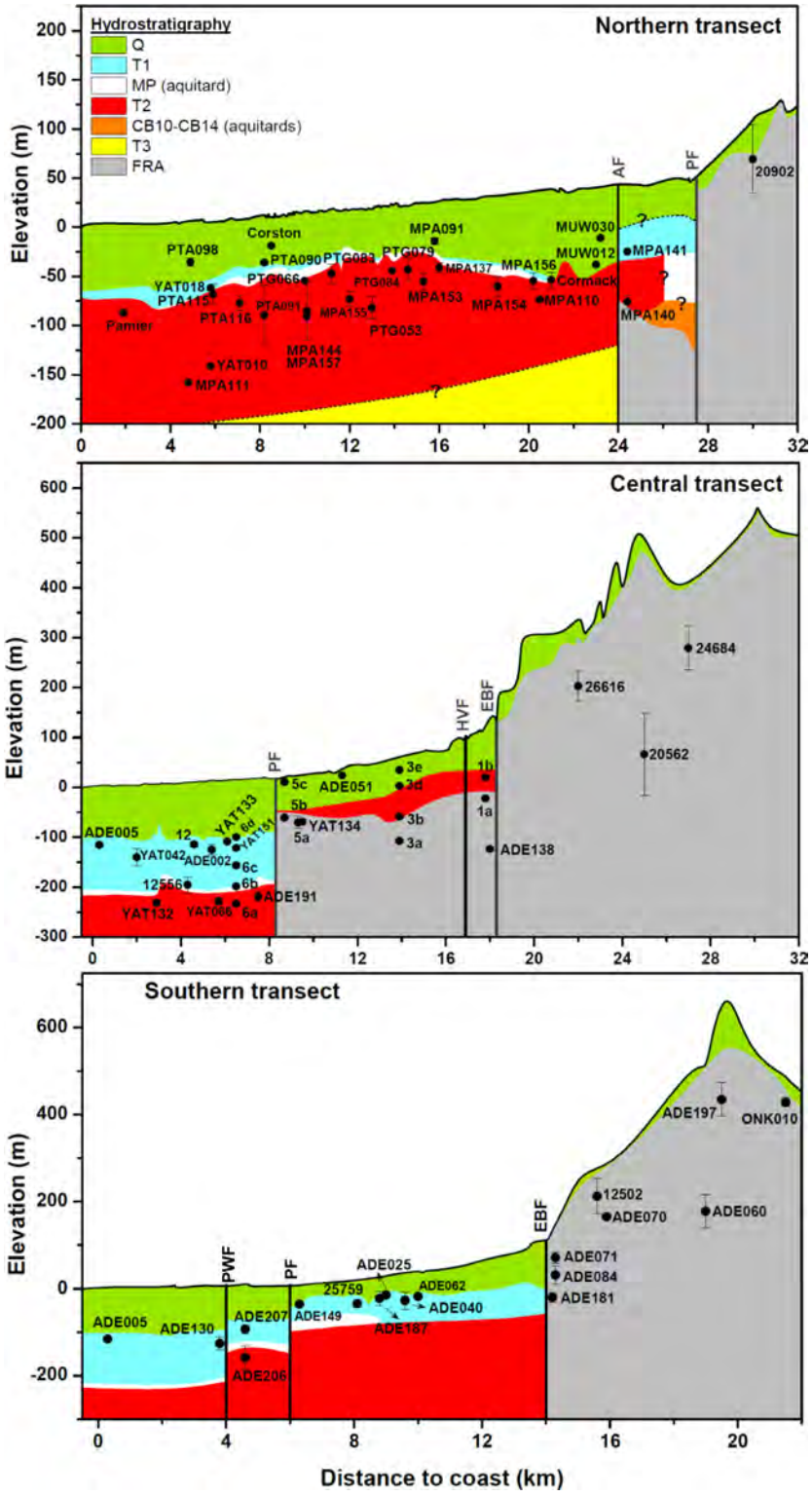

Fig. 3. Schematic hydrogeological cross sections of the (a) Northern, (b) Central, and (c) Southern Transects. Screen intervals are shown using vertical error bars, only when screen lengths exceed the size of the symbols. Q: Quaternary aquifer; T1: Tertiary 1 aquifer; T2: Tertiary 2 aquifer; FRA: Fractured aquifer; MP: Munno-Para aquitard. AF: Alma Fault; PF: Para Fault; PWF: Para West Fault; EBF: Eden-Burnside Fault; HVF: Hope Valley Fault.

and Natural Resources (DEWNR). Drilling locations were selected based on existing drillhole information, geological maps, hydrostratigraphy, ease of access and minimal disturbance to residents in an urban environment. The new monitoring wells were designed and constructed to target the three major aquifer systems (T1, T2 and FRA) and completed with short screen intervals so that a representative sample could be collected from a discrete interval within the aquifer of interest (wells within each nest are designated a, b, c, d and e in order of decreasing depth). Well development was performed using compressed air at least 5 m above the top of screen to minimize the potential for contamination of groundwater with atmospheric air.

Groundwater sampling was conducted at 54 wells (14 new drilled and 40 existing monitoring wells) across the Adelaide Plains and MLR region between October 2013 and June 2015 (Fig. 4). Sampled wells are mostly located along three transects, each of which extends from the Western MLR across the Plains to the coast. Although samples were also collected from the Q aquifer, the T1, T2 and FRA aquifers were primarily targeted. The groundwater sampling program supplements previous environmental tracer studies in the Southern and Central parts of the aquifer system (Dighton et al., 1994; Gerges, 1999), in the Northern Adelaide Plains (Baird, 2010) and in the MLR (Green et al., 2010). In this paper we present and discuss data from new and previous sampling campaigns. Among the 54 sampled wells in this study, 14 wells had been sampled previously for environmental tracer concentrations. Because results were very similar to previous studies, only results from the latest sampling (this work) are provided for these 14 wells.

A YSI® multi-parameter probe was used to measure pH, specific electrical conductivity (SEC) and temperature during purging of the monitoring wells using a flow-through cell. Alkalinity (as $CaCO_3$) and dissolved oxygen (DO) were measured in the field using HACH titration kits. Prior to sampling, the static water level was measured from top of casing (TOC) using an electric water level indicator. Groundwater samples were collected after purging three well volumes or once the physical parameters of temperature, SEC and pH did not change by more than 5% within a half hour period.

Groundwater samples for analyses of major ions and trace elements were collected in 50 mL polyethylene bottles. Samples were filtered (0.45 μm) and samples for cation analysis were acidified with concentrated HNO_3 in the field. Samples for water stable isotope ratios ($^2H/^1H$, $^{18}O/^{16}O$) were collected in 2 mL glass vials in duplicate. Samples for carbon isotopes ($^{13}C/^{12}C$) and radiocarbon (^{14}C) were collected in 1 L plastic bottles, unfiltered with zero head

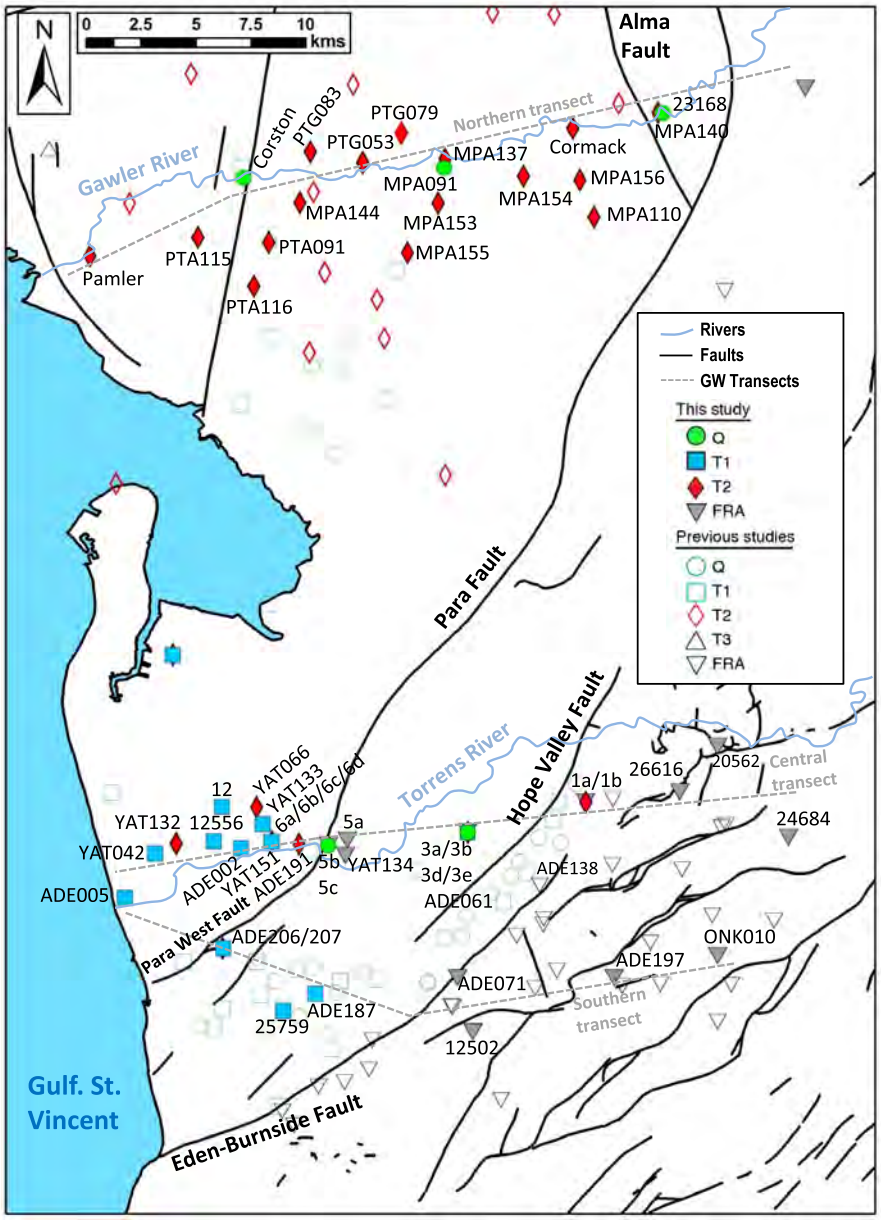

Fig. 4. Wells sampled during the present (filled symbols) and previous (hollow symbols) studies. Only wells sampled during this study are labelled.

space and no preservative. Samples for dissolved gases (^{4}He, ^{20}Ne, ^{40}Ar and N_2) were collected using passive gas diffusion samplers (Gardner and Solomon, 2009) installed at the screen depth for a minimum of seven days or collected in copper tubes during well sampling (Weiss, 1970). Dissolved gas concentrations (^{4}He, ^{40}Ar and N_2) in groundwater were also measured in-situ from a number of the groundwater wells using a portable Gas-Equilibrium Membrane Inlet Mass Spectrometer (GE-MIMS) (Brennwald et al., 2016).

4.2. Analytical procedures

Major cations (Na^+, K^+, Mg^+, Ca^{2+}), and trace elements (Sr^{2+}, Br^-) were analyzed by Inductively Coupled Plasma Optical Emission Spectrometry (Spectro ARCOS), and anions (Cl^-, SO_4^{2-}, NO_3^-, HCO_3^-) by ion chromatography (Dionex ICS-2500). All ions analyses were performed at the Commonwealth Scientific and Industrial Research Organization (CSIRO), Analytical Chemistry Unit in Adelaide (Australia). Ion balances were typically better than ±5%.

Water stable isotopes were measured using a Picarro L2130-i $\delta^{18}O/\delta^2H$ Ultra High Precision Isotopic Water Analyser (School of the Environment, Flinders University, Adelaide, South Australia). Results are reported as a deviation from the Vienna Standard Mean Ocean Water (SMOW) in per mil (‰) difference using delta (δ) notation. The analytical precision for $\delta^{18}O$ and δ^2H is ±0.025‰ and ±0.1‰, respectively.

Radiocarbon was analyzed using Accelerator Mass Spectrometry (AMS) (Rafter Radiocarbon Laboratory, GNS Science, Lower Hutt, New Zealand), and stable carbon isotopes ratio ($^{13}C/^{12}C$) was measured using an Isotope Ratio Mass Spectrometer (Stable Isotope Laboratory, GNS Science, Lower Hutt, New Zealand). Stable carbon isotopes are reported in delta notation ($\delta^{13}C$; ‰) relative to the Pee Dee Belemnite (PDB) standard, and carbon-14 activities are reported as percent modern carbon (pmC) according to the convention described in Stuiver and Polach (1977). The measured apparent ^{14}C activities ($^{14}C_{uncorr}$) on TDIC (Total Dissolved Inorganic Carbon) were corrected ($^{14}C_{corr}$) for carbonate dissolution as follows (Clark and Fritz, 1997):

$$^{14}C_{corr} = {}^{14}C_{uncorr}\frac{\delta^{13}C_{rech} - \delta^{13}C_{carb}}{\delta^{14}C_{TDIC} - \delta^{14}C_{carb}} \quad (1)$$

where $\delta^{13}C_{TDIC}$ is the measured $\delta^{13}C$ activity on TDIC, $\delta^{13}C_{rech}$ is the assumed initial $\delta^{13}C$ ratio in groundwater recharge and $\delta^{13}C_{carb}$ is the $\delta^{13}C$ ratio of carbonate in the aquifer matrix, assumed to be 0‰ (Clark and Fritz, 1997).

Dissolved gases collected in copper tubes or diffusion cells were analyzed at the CSIRO Environmental Isotope Laboratory (Adelaide, South Australia) with a Stanford Research Systems RGA 220 quadrupole mass spectrometer with cryogenic separation (Poole et al., 1997) (^{4}He and ^{40}Ar precision ±5%, ^{20}Ne and N_2 precision not reported). Dissolved gas concentrations were also measured in the field, using a portable GE-MIMS system (Brennwald et al., 2016). This system is based on the earlier GE-MIMS concept (Mächler et al., 2012, 2013, 2014), but is more compact and portable, and able to measure dissolved gases in a stream of water quasi-continuously (every 12 min) with a precision of better than 4% for ^{4}He and 1% for ^{40}Ar and N_2. The GE-MIMS system was connected to the pump outlet at the start of well purging, although the reported results represent an average of the last six measurements after the well had been purged and stable conditions had been reached. ^{4}He concentrations measured using laboratory and field-based methods agreed within less than 10%, and so only GE-MIMS measurements are reported where both results are available. (concentrations of ^{40}Ar, ^{20}Ne and N_2, were measured but are not reported in this study)

5. Results

5.1. Major ions

The salinity (using Total Dissolved Solids, TDS, as a proxy of it) of groundwater samples ranges between 130 and 8700 ppm TDS. Most samples are sodium-chloride type (Fig. 5), and Ca, Mg and HCO_3 concentrations are observed to be clearly above the seawater dilution line (Fig. S2), indicating that additional sources for Ca and Mg, other than seawater, may exist (e.g., dissolution of gypsum and carbonates). Saturation indices of calcite and dolomite are both above saturation (Table S1), while gypsum is below saturation, suggesting that carbonate dissolution prevails over gypsum dissolution as a source of Ca and Mg to groundwater. Furthermore, the correlation between SO_4 and Cl is rather weak (R^2 = 0.38) and SO_4/Cl ratios are low (between 0.16 and 0.24 in all aquifers), indicating that gypsum dissolution plays only a minor role in groundwater chemistry. Groundwater-rock interactions therefore significantly affect the chemistry of groundwater in the Adelaide Plains region. A complete chemistry dataset for all sampled wells can be found in Table S2.

Nitrate (NO_3^-) concentrations are relatively high in most Q wells sampled, reaching up to 138 mg L^{-1} in the Northern Transect (Fig. 6), most probably due to return flow from agricultural irrigation. Nitrate concentrations in the T1 aquifer are generally below 10 mg L^{-1}, occasionally reaching concentrations close to 30 mg L^{-1} (Well Canala, Northern Transect) and 55 mg L^{-1} (Well 3d, Central Transect). In the Northern Transect these T1 concentrations can be due to leakage from the overlying Q aquifer, but in the Central Transect such high and isolated concentration is likely to be caused by sewage leakage. Nitrate concentrations in the T2 aquifer are systematically close to the detection limit or undetectable. Groundwater in the FRA aquifer is generally close to the detection limit, and only occasional concentrations of 6 mg L^{-1} (ADE092) and up to 31 mg L^{-1} (well 6883) were measured (Fig. 6), likely due to infiltration of return flow from local agricultural practices and/or contamination of septic tanks from isolated households.

Chloride concentrations increase towards the coast in all three transects and concentrations in the Q aquifer are generally close to or higher than concentrations in aquifers T1, T2 and FRA (Fig. 7). This suggests high rates of evapotranspiration from the shallowest aquifer and likely low vertical infiltration from the Q to lower T1 and T2 aquifers. However, it does not rule out the possibility that the Tertiary aquifers are a mixture of water from both the FRA and Q aquifers.

Mean Cl concentrations in each transect were calculated combining data from this work, previous studies and historical data from the DEWNR. Significant variation exists in the Q aquifer between the Northern transect (1300 mg L^{-1}, n = 65; n: number of samples) and the Central and Southern Transects (650 mg L^{-1}, n = 198). Mean Cl concentration in the FRA aquifer in the MLR is approximately 290 mg L^{-1} (n = 300), while in the Northern Transect mean chloride concentration in the MLR is significantly higher, 1200 mg L^{-1} (n = 74). Mean Cl concentrations in the T1 and T2 aquifers are relatively constant in all three transects, approximately 500 mg L^{-1} (n = 500) and 700 mg L^{-1} (n = 257), respectively. The only groundwater sample available from the T3 aquifer from previous works has a concentration of approximately 5000 mg L^{-1}. Nevertheless, few historical data from the T3 aquifer show concentrations of up to 80,000 mg L^{-1}.

5.2. Stable isotopes and radiocarbon

Stable isotopes (^{18}O, ^2H) can provide valuable information on groundwater recharge processes because their composition

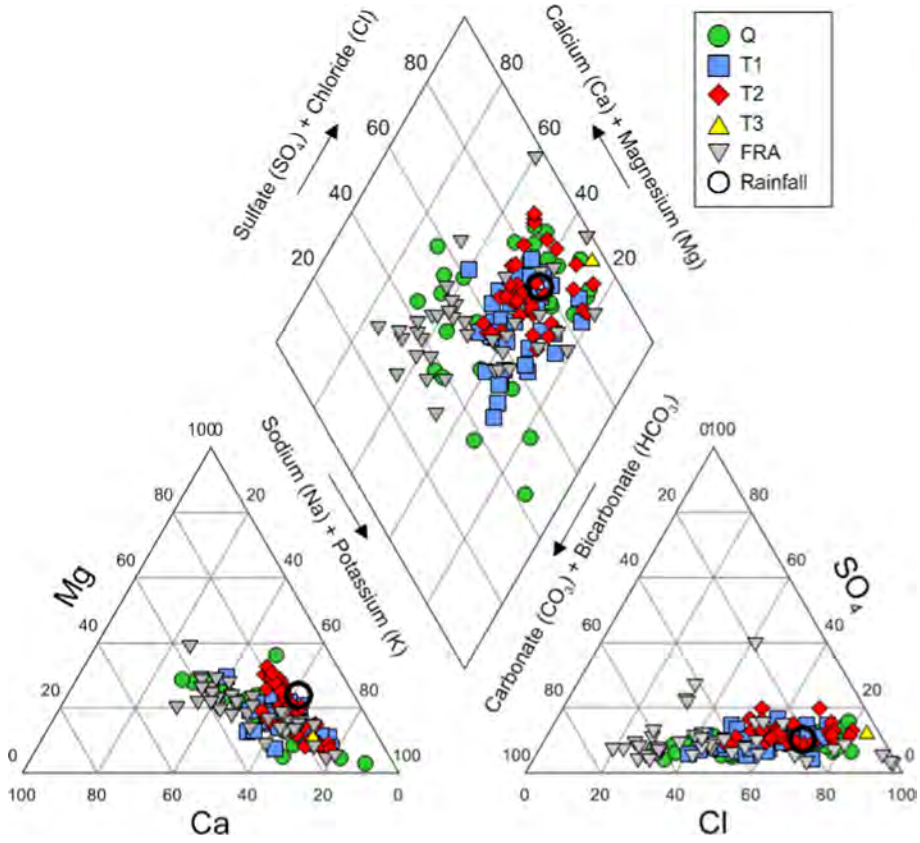

Fig. 5. Piper diagram, highlighting the Na-Cl type of waters. Groundwater samples from the present and previous studies are used. Rainfall composition in the Adelaide Plains (~40 m asl) is from Crosbie et al. (2012).

records the atmospheric conditions at the time of recharge (Gat, 1996). The amount-weighted mean $\delta^{18}O$ and $\delta^{2}H$ ratios in the Adelaide Plains (~40 m asl) rainfall between 2008 and 2010 are −4.1‰ and −19.1‰, respectively (Crosbie et al., 2012). Rainfall isotopic composition shows a significant elevation (and consequently temperature) effect, becoming depleted towards the Mount Lofty Ranges, with −5.1‰ and −24.3‰ at 160 m asl, and −7.6‰ and −44.1‰ at 435 m asl, for ^{18}O and ^{2}H respectively (as measured between 2009 and 2011, Guan et al., 2013). Groundwater in the Adelaide Plains has $\delta^{18}O$ values ranging from −6‰ to −3‰ and $\delta^{2}H$ ranging from −32‰ to −16‰ (Fig. 8). In general, groundwater samples from the Q and FRA aquifers are located along the LMWL (Local Meteoric Water Line; Liu et al., 2010), although some Q samples are shifted towards the right of the line (less negative δ values; water enriched in heavier O and H isotopes), suggesting evaporative enrichment during recharge. Samples from the FRA aquifer are more depleted (isotopic composition shifted towards more negative δ values), indicating that these waters are more enriched in lighter O and H isotopes than those from Q aquifers, which is consistent with an origin within the Western MLR. Groundwater samples from the T2 aquifer are located along a line approximately parallel to the LMWL but shifted towards the right, suggesting that groundwater in the T2 aquifer has a different origin than present rainfall. T2 samples closer to the coast are located towards more negative δ values, while samples closer to the Western MLR are located in the opposite edge of that line, towards less negative δ values. This trend, in combination with the elevation and temperature effects on rainfall isotopic composition, suggests that groundwater in the T2 aquifer close to the coast has a palaeometeoric origin (possibly recharged during the last cold period; >12,000 y) (Varsányi et al., 1997). As distance from the coast increases, the water becomes more enriched, suggesting that was recharged during a warmer climate (<12,000 y). Groundwater samples from the T1 are scattered along the LMWL, between the Q and FRA samples. Samples 5a, 5b and YAT134 are highly depleted in ^{2}H, and also were characterized by high Cl concentrations (Fig. 7b). The only groundwater sample available from the T3 aquifer is isotopically light ($\delta^{18}O$ −4.55‰, $\delta^{2}H$ −26.5‰).

An analysis of ^{18}O with distance (Fig. 9) confirms an isotopic depletion in T1 and T2 aquifers west of the PF in the Northern and Central Transects. The ^{18}O composition of these aquifers in the Southern Transect is nearly constant. Groundwater in the Q aquifer becomes enriched towards the coast in all three transects, although this is more visible in the Central and Southern Transects. In the Central and Southern Transects, samples from the FRA aquifer west of HVF and EBF faults are enriched compared to samples east of these faults. Overall this suggests ongoing evapotranspiration processes in the Q aquifer, probable little influence of vertical Q infiltration into the Tertiary aquifers T1 and T2, and possible infiltration of Q aquifer into the FRA aquifer near the HVF and EBF faults.

Considering valid the current accepted conceptual model of the Adelaide Plains groundwater system (T1 and T2 aquifers mainly recharged with rainfall in the MLR that infiltrates into the FRA aquifers; see details in Section 3), it is possible to calculate the contribution of Q and FRA into the T1 aquifer using mean values of $\delta^{2}H$ in mass balance calculations for the Central and Southern transects. Results suggest that the Q aquifer would contribute around 25% to the T1, with the remaining contribution from the FRA aquifer. This calculation is not possible for the T2 aquifer, because the

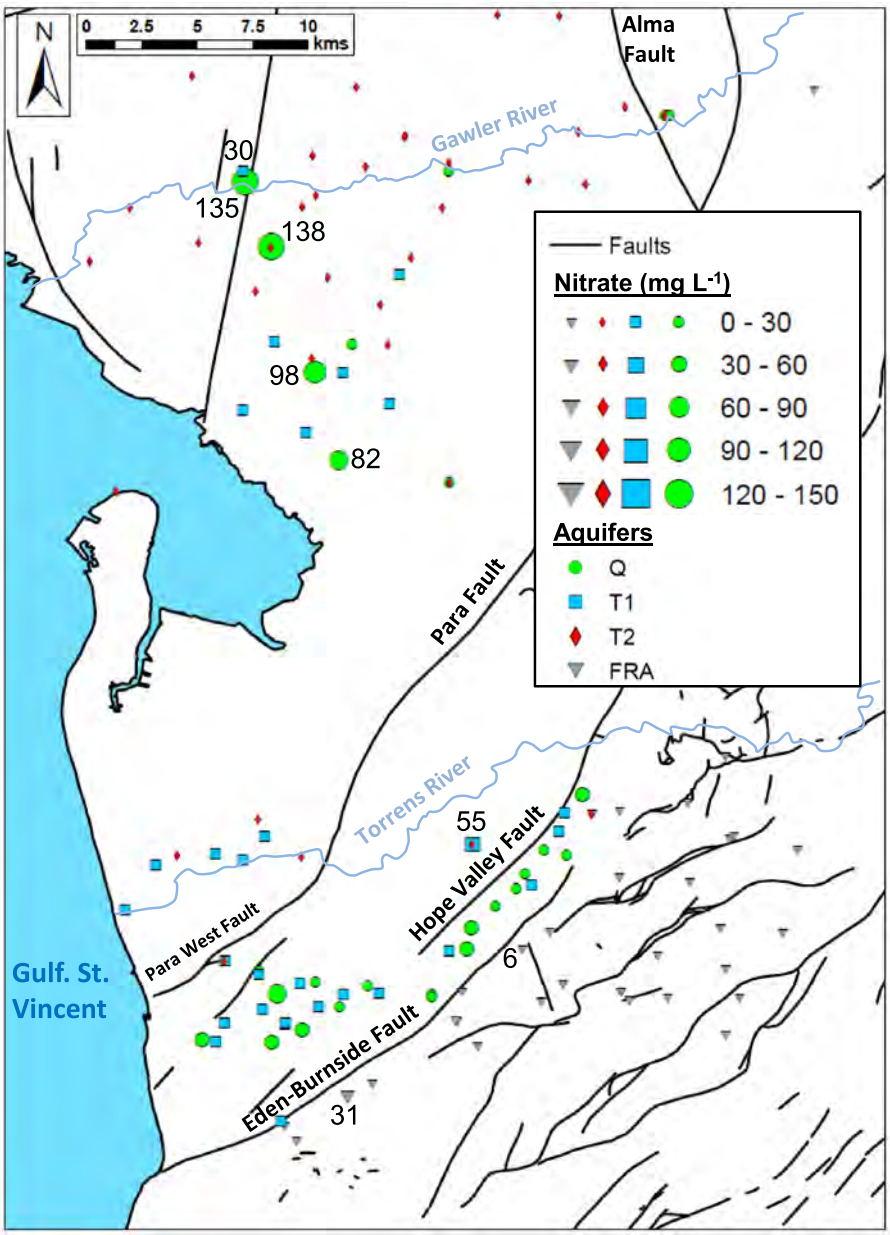

Fig. 6. Nitrate concentrations in the Adelaide Plains groundwater system during the present and previous studies. Only the highest concentrations are labelled.

water appears to reflect recharge under a different climate. In the Northern Transect there is not enough data from the FRA aquifer to calculate mixing fractions.

$\delta^{13}C$ values in groundwater samples range from −15.2 to −2.8‰, and $^{14}C_{uncorr}$ activities range from 0.4 to 91 percent modern Carbon (pmC, Fig. 10). Samples with low ^{14}C activities are generally more enriched in ^{13}C, suggesting that the decrease of ^{14}C activity by radioactive decay is enhanced by dissolution of dead marine carbonate minerals (0‰; Pearson and Hanshaw, 1970). None of the samples from the Q and FRA aquifers are very enriched in ^{13}C (−15.2 to −8.6‰), with an average of −11.3 ± 0.7‰, which is in good agreement with the often assumed $\delta^{13}C_{rech}$ in groundwater recharge of −12‰ (Clark and Fritz, 1997). Based on the current conceptual model of the region (see details in Section 3), groundwater in the Adelaide Plains is believed to be recharged from the Q and FRA aquifers, and we thus apply a $\delta^{13}C_{rech}$ value of −11.3‰ in Eq. (1).

The calculated $^{14}C_{corr}$ values in the Q aquifer are mostly between 65 and 115 pmC (~4000 y – modern), with the exception of one sample at approximately 11 km (well ADE051) that has an age of ~28,000 y. This is significantly older than what would be expected for the Q aquifer, and it would be necessary to resample this well to confirm the result. $^{14}C_{corr}$ ages tend to increase with depth and distance from the Western MLR within T1 and T2 aquifers (Fig. 11). Some high $^{14}C_{corr}$ activities were measured at significant depths (screens at depths up to 280 mbg; meters below ground) and close to major faults (Fig. 11). In particular, in the Northern Transect, $^{14}C_{corr}$ activities of 88.5 and 81.0 pmC (~1000 to 2000 y) were measured on MPA140 (screened at 112–125 mbg and 88–101 mbwt –meter below water table; T2 aquifer) and MUW030 (screened at 46–50 mbg and 23–27 mbwt; T2 aquifer), respectively. In the Central Transect, 70.5 pmC (~3000 y) was measured on ADE138 (277–287 mbg and 168–178 mbwt; FRA aquifer), and in the Southern Transect, 66.0 and 61.8 pmC (~3000–4000 y)

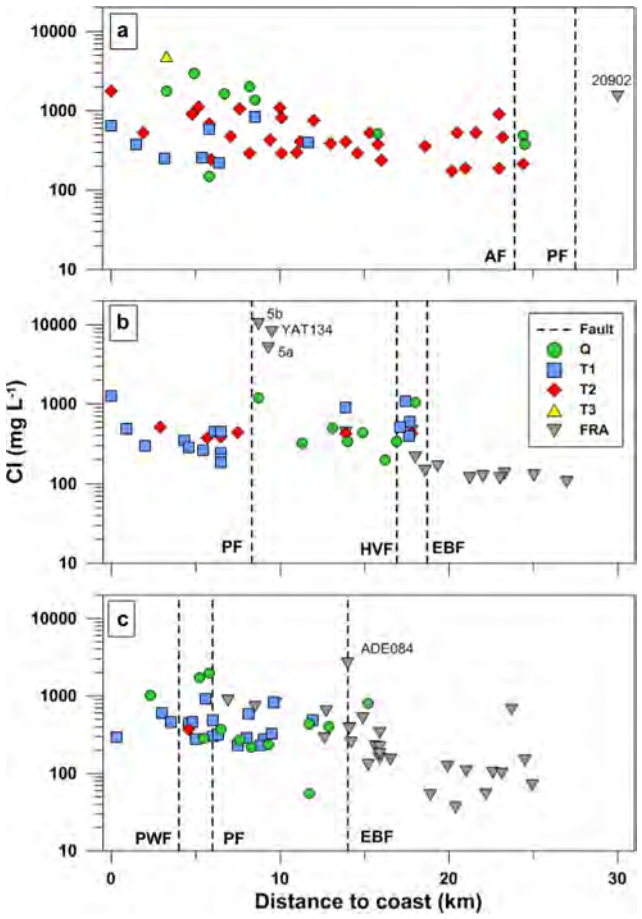

Fig. 7. Cl concentrations increase towards the coast in the Adelaide Plains aquifer system, and concentrations in the Q aquifer are generally close to or higher than concentrations in aquifers T1, T2 and FRA, suggesting high rates of evaporation from the Q aquifer. (a) Northern Transect; (b) Central Transect; (c) Southern Transect. AF: Alma Fault, PF: Para Fault; PWF: Para West Fault; EBF: Eden-Burnside Fault; HVF: Hope Valley Fault.

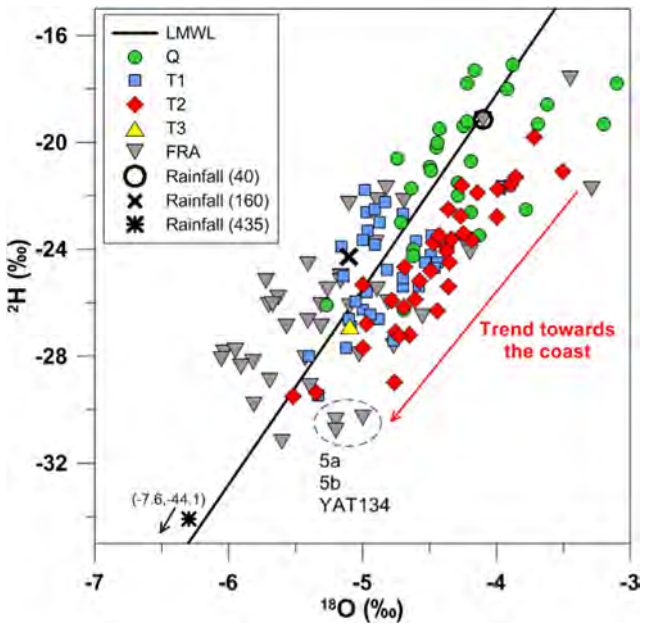

Fig. 8. Relationship between ^{18}O and ^{2}H values in groundwater (LMWL: Local Meteoric Water Line $\delta^2H = 7.3\delta^{18}O + 11$, Liu et al. (2010)). Average-weighted rainfall composition in the plains (40 m asl) from Crosbie et al. (2012), in the hills (160 and 435 m asl) from Guan et al. (2013). Samples from the T2 aquifer follow a line nearly parallel to the LMWL. T2 samples are lighter (towards negative values) closer to the coast, and heavier (towards less negative values) closer to the Western MLR.

were measured on ADE071 (37–62 mbg, depth to water table could not be measured at the sampling time; FRA aquifer) and ADE084 (18–60 mbg and 3–45 mbwt; FRA aquifer), respectively. This data suggests deep infiltration of modern water along the major faults.

Although Fig. 11 groups together wells screened at different depths, an increase in age along the flow line is apparent, particularly in the T2 aquifer in the Northern Transect and in the T1 aquifer in all three transects. Considering all wells west of AF in the Northern transect, and ignoring variation in screen depths, the T2 aquifer shows an increase in $^{14}C_{corr}$ ages towards the coast, from 2000 to 4000 years at distances between 20 and 24 km to 32,000–33,000 years at distance of 2–6 km (confirming the palaeometeoric origin of water in the T2 aquifer, as suggested by the analysis of stable isotopes). An increase in age with distance is not usually observed within unconfined aquifers (Cook and Bohlke, 2000; Vogel, 1970), and this suggests that the T2 aquifer is at least partially confined, and receives a significant volume of its recharge from the Western MLR. Although less apparent, an increase in age with depth can be observed in some areas. For example, between 13 and 14 km distance, a groundwater age of 6000 years was measured at a screen depths between 51 and 72 mbg (well PTG084), and 29,000 years at a screen depth of 95–118 mbg (well PTG053). Although carbon-14 data for the T1 aquifer is quite sparse, groundwater age increases from 9000 years at 12 km to 28,000 years at 1.5 km. There is not enough data in the T1 aquifer to evaluate variations in age with depth.

Age trends in the Central Transect are less immediately apparent from Fig. 11, as the density of sampling is lower, and age is affected both by distance along the transect and depth of screened intervals. A piezometer nest (6d, 6c, 6b and 6a) at 6.5 km from the coast, shows an increase in $^{14}C_{corr}$ age from ~10,000 y at a screen depth of 111–117 mbg (well 6d; T1 aquifer) to 27,500 y at 212–218 mbg (well 6b; T1 aquifer) and ~30,000 y at a screen depth of 245–251 mbg (well 6a; T2 aquifer). Near the top of the T1 aquifer, the age increases towards the coast from approximately 8000–23,000 years at 5.4–6.5 km (wells ADE002, ADE133 and YAT151; screened in the top 10–30% of the aquifer thickness) to 25,000–31,000 years at 0.3–2 km (wells ADE005 and YAT042; screened in the top 10–40% of the aquifer thickness). A single sample in the T1 aquifer east of the PF had an age of 2000 years. West of the PF in the T2 aquifer, $^{14}C_{corr}$ ages range between ~23,000 and 30,000 y at 2.9–7.5 km distance from the coast. There is a clear relationship between $^{14}C_{corr}$ age and screen depth, with the deepest well having the oldest measured $^{14}C_{corr}$ age (well 6a, 245–251 mbg, ~30,000 y), and the shallowest well having the youngest $^{14}C_{corr}$ age (well ADE191, 226–246 mbg, ~23,000 y). East of the PF only two samples in the T2 aquifer are available, with $^{14}C_{corr}$ ages of ~26,000 y at 14 km (well 3b) and ~9000 y at 18 km from the coast (well 1b).

In the Southern Transect west of the PWF, only two samples are available, with ~16,000 y at 2.1 km (well ADE130) and ~31,000 y at 0.3 km (well ADE005), both in the top 30% of the aquifer thickness. East of the PF, samples in the top 20% of the aquifer thickness have $^{14}C_{corr}$ ages between ~10,000 and 15,000 y at distances of 7.9 and 3.5 km, respectively (wells ADE062 and ADE149). Near the middle of the aquifer $^{14}C_{corr}$ ages of ~13,000 y were measured at distances between 8.1 and 9.6 km (wells 25759 and ADE040). Between the PWF and PF, at 4.6 km, one sample had a $^{14}C_{corr}$ age of ~9000 y (well ADE207). A single sample in the T2 aquifer in the Southern Transect, between the PWF and PF, had a $^{14}C_{corr}$ age of ~21,000 y (well ADE206).

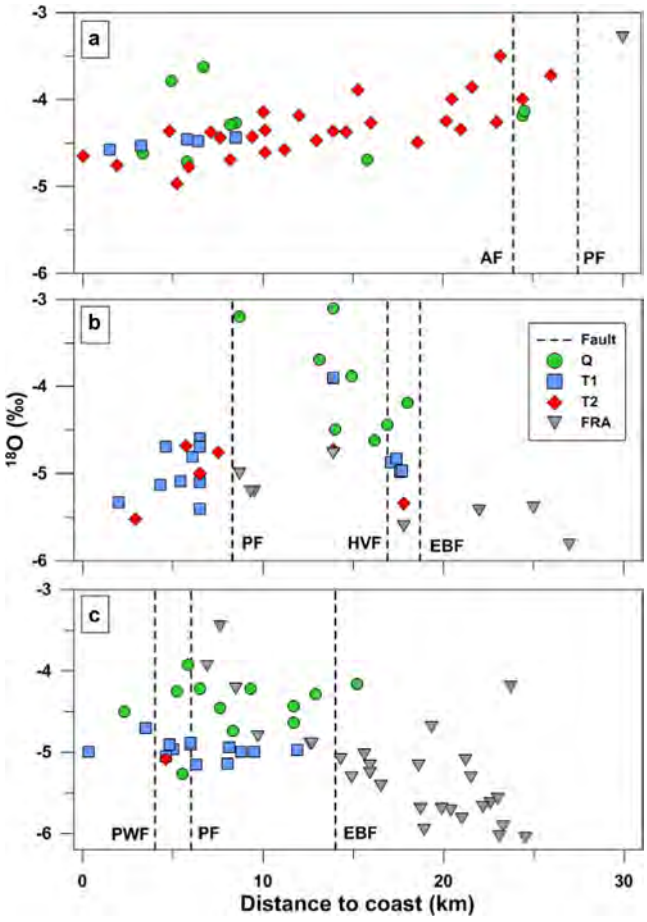

Fig. 9. Distribution of ^{18}O with distance to coast in the (a) Northern; (b) Central; and (c) Southern Transects. Groundwater in T1 and T2 becomes enriched towards the Mount Lofty Ranges, while groundwater in the Q aquifer generally becomes enriched towards the coast.

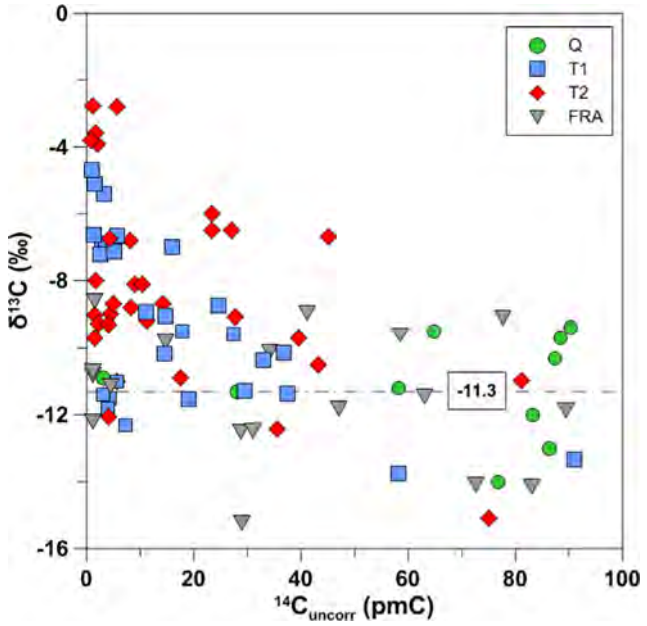

Fig. 10. δ^{13}C (‰) vs $^{14}C_{uncorr}$ (pmC) in the Adelaide Plains aquifer system. Groundwater samples from the present and previous studies are used. An average δ^{13}C of −11.3 ± 0.7 is calculated for the Q and FRA aquifers, the two aquifers from where recharge to Tertiary aquifers is believed to occur in the Adelaide Plains system.

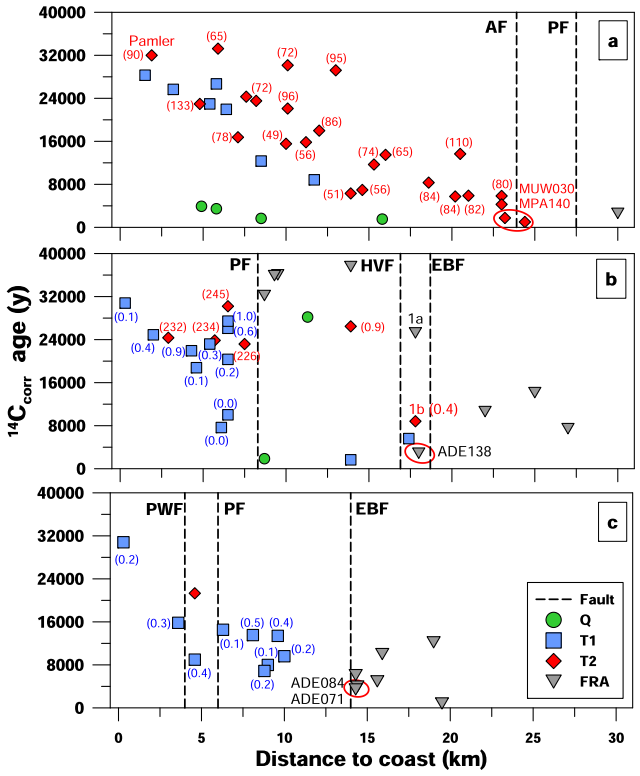

Fig. 11. Relationship between $^{14}C_{corr}$ age and distance to coast in the (a) Northern; (b) Central; and (c) Southern Transects. Radiocarbon age generally increases towards the coast in the Adelaide Plains (particularly visible in the T2 aquifer in the Northern Transect). Numbers in brackets are the relative depths of the top of the screen length (0 = top of the aquifer; 1 = bottom of the aquifer). When the bottom of the aquifer is unknown (T2 aquifer west of AF and PF in the Northern and Central Transects), numbers in brackets denote absolute depths (mbg) of the top of the screen. Symbols with red circles highlight samples where younger groundwater than expected was found close to major faults at relatively important depth (up to 280 mbg in ADE138). AF: Alma Fault, PF: Para Fault; PWF: Para West Fault; EBF: Eden-Burnside Fault; HVF: Hope Valley Fault.

5.3. Dissolved gases

Based on recharge temperatures between 2 and 30 °C and up to 0.01 cm^3 g^{-1} of excess air, ^{4}He concentrations at equilibrium should be between 4.35×10^{-8} cm^3 g^{-1} and 9.99×10^{-8} cm^3 g^{-1}. Only values for four samples (wells 1b, 3b, 12 and ADE207) fall within this range, with the other samples having ^{4}He concentrations up to four orders of magnitude higher (Fig. S3). This means that most ^{4}He concentrations in the groundwater cannot be explained by equilibrium with atmospheric ^{4}He at the time of recharge, and that subsurface production or accumulation of ^{4}He is the main contributing processes within the aquifer.

The distribution of ^{4}He along the three transects is shown in Fig. 12. In the Northern Transect, considering only those samples west of the AF (thus excluding MPA140), there is an increase in ^{4}He concentration of one order of magnitude over 20 km in the T2 aquifer, approximately 1.7×10^{-7} cm^3 STP g^{-1} km^{-1} (Fig. 12a). In the Central Transect, ^{4}He concentrations west of the PF in the T2 aquifer increase from 7.6×10^{-7} cm^3 STP g^{-1} in ADE191 to 4.3×10^{-6} cm^3 STP g^{-1} in YAT132, over a distance of 5 km, approximately 7.1×10^{-7} cm^3 STP g^{-1} km^{-1}, four times higher than the Northern transect (Fig. 12b). Concentrations in the T1 aquifer in the Central Transect (only available west of PF) are nearly constant at around 3×10^{-7} cm^3 STP g^{-1}, with one sample (well 12) with a much lower concentration (4.9×10^{-8} cm^3 STP g^{-1}). In the Southern Transect there is insufficient data on ^{4}He to identify any trend (Fig. 12c).

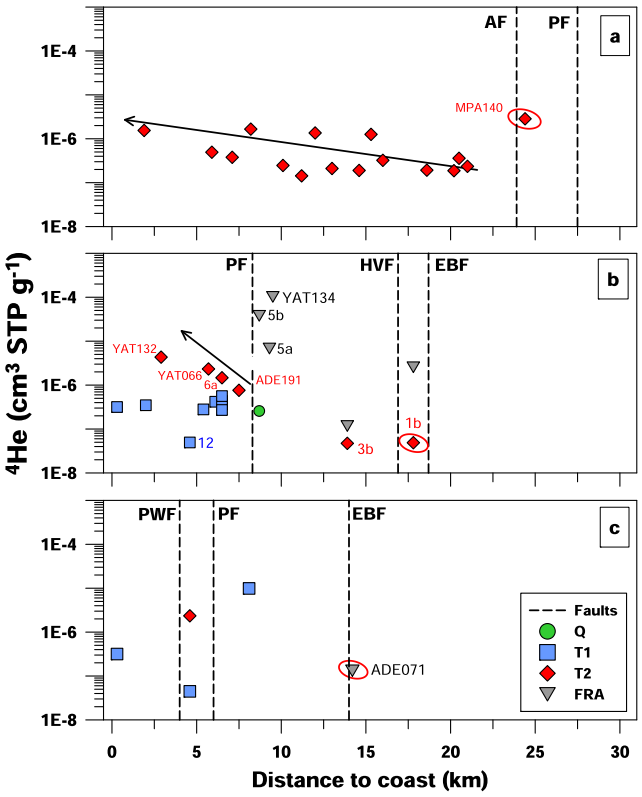

Fig. 12. Distribution of ^{4}He concentrations with distance to coast in (a) Northern; (b) Central; and (c) Southern Transects. Helium-4 concentrations increase in the T2 aquifer in the Northern transect and west of PF in the Central transect, but with a higher slope by a factor of four in the Central Transect (arrows show the trend of that increase). Symbols with red circles highlight groundwater samples where high $^{14}C_{corr}$ activities were measured close to faults, at relatively important depths. AF: Alma Fault, PF: Para Fault; PWF: Para West Fault; EBF: Eden-Burnside Fault; HVF: Hope Valley Fault. (For interpretation of the references to colour in this figure legend, the reader is referred to the web version of this article.)

The relationship between ^{4}He and $^{14}C_{corr}$ ages in the T1 and T2 aquifers allows us to define lower (8×10^{-12} cm^3 STP g^{-1} y^{-1}) and upper (1×10^{-10} cm^3 STP g^{-1} y^{-1}) bounds of the ^{4}He accumulation rate (Fig. 13). With the exception of MPA140 (T2 aquifer Northern Transect), this range of accumulation rates can explain most of the data from the Adelaide Plains. It is interesting to note that ^{4}He concentration in the T1 aquifer in the Central Transect is nearly constant at around 3×10^{-7} cm^3 STP g^{-1}. This may be due to a lower production rate for the T1 aquifer (compared to the T2). It is also likely that the Munno Para clay aquitard that overlays the T2 aquifer shields the T1 aquifer from receiving upward diffusion of ^{4}He from deeper layers, also contributing to build up the helium concentration in the T2 aquifer below.

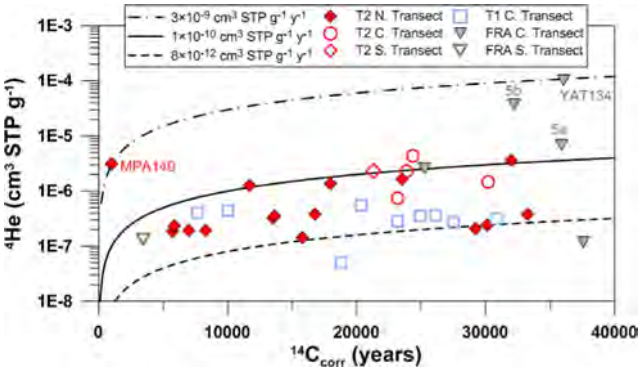

Fig. 13. Relationship between ^{4}He concentrations and $^{14}C_{corr}$ ages for the T1, T2 and FRA aquifers. Best fits of upper (1×10^{-10} cm^3 STP g^{-1} y^{-1}) and lower (8×10^{-12} cm^3 STP g^{-1} y^{-1}) ^{4}He accumulation rates for wells west of AF and PF are shown. The sample east of AF (MPA140), in the Northern Transect, can only be fitted with a much higher accumulation rate of 3×10^{-9} cm^3 STP g^{-1} y^{-1}, similar to deep and highly saline FRA groundwater from wells 5b and YAT134. Helium-4 concentrations in the T1 aquifer are relatively constant, so no accumulation rate curve can be fitted.

The high concentration measured in well MPA140 is most probably due to a mixing young and old groundwater. Mixing of a small amount of very old water into samples of younger water will have little to no effect on ^{14}C age, because the ^{14}C activity of waters older than 40,000 years is close to zero. Three groundwater samples from the FRA aquifer (5a, 5b and YAT134), located just east of the PF in the Central Transect, are also characterized by high ^{4}He concentrations (1×10^{-5}–1×10^{-4} cm^3 STP g^{-1}) (Fig. 14a). These three groundwater samples also have high Cl concentrations (5000–10,000 mg L^{-1}) and very old $^{14}C_{corr}$ ages (>30,000 y) (Fig. 14b). However not all samples at significant depths next to faults have these characteristics. For example, samples from MPA140 (T2 aquifer), 1b (T2 aquifer), and ADE071 (FRA aquifer), all close to faults, have ^{4}He concentrations ranging between 3.1×10^{-6} cm^3 STP g^{-1} and 4.9×10^{-8} cm^3 STP g^{-1}, but all of them have very low Cl concentrations ($\leqslant$400 mg L^{-1}). This suggests that groundwater from wells 5a, 5b and YAT134 may have a different source to groundwater from other wells close to the faults, most likely old brine.

5.4. Groundwater flow velocities

The increase in $^{14}C_{corr}$ ages in the T2 aquifer with distance from the Western MLR (see Section 5.2 and Fig. 11) was used to calculate flow velocities. In the Northern Transect flow velocities between 0.3 and 1.8 m y^{-1} were calculated, with a mean flow velocity of

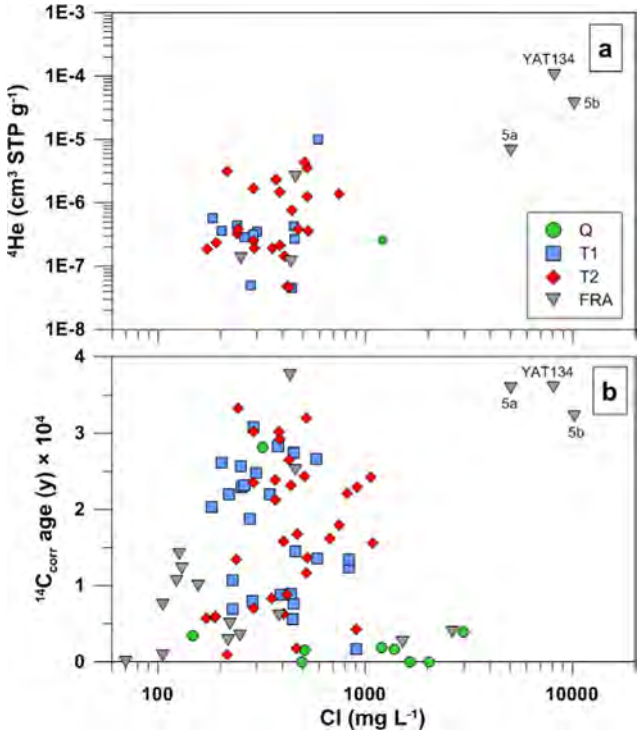

Fig. 14. Relationship between dissolved ^{4}He concentrations and (a) $^{14}C_{corr}$ ages, and (b) Cl concentrations. FRA samples 5a, 5b and YAT134, located east to the PF in the Central Transect, consistently present high Cl concentrations, very low $^{14}C_{corr}$ activities and high ^{4}He concentrations, suggesting influence of very old brines.

0.8 m y^{-1} (24 km in 30,000 years). Carbon-14 data for the T1 aquifer is quite sparse, but groundwater velocities between 0.5 and 0.8 m y^{-1} can be estimated (5–10 km in 6000–20,000 years).

In the Central Transect, west of PF in the T2 aquifer, a flow velocity cannot be estimated because: (1) the low density of sampling in that area; (2) the vertical variation in screen depth; and (3) $^{14}C_{uncorr}$ activities are very low (<2 pmC), close to the detection limit of ^{14}C. In the T1 aquifer west of PF, horizontal velocities between 0.2 and 0.6 m y^{-1} are estimated from wells in the top T1 aquifer (6 km in 10,000–21,000 years). In the Southern Transect data is too sparse to reliably estimate a horizontal flow velocity. Overall, in the Adelaide Plains horizontal flow velocities can be estimated west of the PF, but there is not enough data to estimate flow velocities east of the PF, and thus, identify whether or not faults cause a change in flow velocity.

Based on a mean helium accumulation rate of 5.4×10^{-11} cm^3 STP g^{-1} y^{-1} in the T2 aquifer in the Northern Transect, an increase in age of 64,000 years over a distance of 20 km is calculated, or a horizontal velocity of approximately 0.3 m y^{-1}, lower but within the same order of magnitude of the mean flow velocity estimated using ^{14}C data (0.8 m y^{-1}). In the Central Transect west of the PF, where radiocarbon velocities could not be estimated, we can use a mean helium accumulation rate of 1×10^{-10} cm^3 STP g^{-1} y^{-1} (Fig. 13), obtaining an increase in age of 35,000 years over a distance of approximately 5 km, or a horizontal velocity of approximately 0.15 m y^{-1}.

6. Discussion

This study has examined environmental tracer data in a complex multilayered aquifer system dissected by faults that cause significant vertical displacement of aquifers. Previous studies that have used environmental tracers to determine apparent groundwater ages, and hence infer flow velocities, have mostly focused on unconfined (Cartwright and Morgenstern, 2012) or confined aquifers (Drimmie et al., 1991; Torgersen et al., 1991). However, the authors are unaware of any previous studies in semi-confined aquifers. In unconfined aquifers, changes in groundwater age mainly occur vertically but not horizontally. In confined aquifers, changes in groundwater age with horizontal distance in the direction of flow are usually much greater than vertical variations in age. In semi-confined aquifers, both vertical and horizontal variations in age are important, and this greatly increases the amount of data that is required to accurately resolve the age distribution. At our field site, this is further complicated by the presence of faults that cause significant vertical displacement of aquifers. Notwithstanding this complexity, the following observations can be made.

6.1. Aquifer recharge

The two main rivers in the area, Torrens and Gawler, are believed to be important sources of recharge for the Quaternary aquifer in the plains, although estimates are unknown. In a recent study Cranswick and Cook (2015) demonstrated that loss of water from streams and creeks in the MLR contribute to the water balance of the Q aquifer with at least 5000 ML y^{-1}. This process was also suggested by fresher water in shallow (<30 m) Q aquifer in the vicinity of creeks and rivers in the Adelaide Plains. However, deeper recharge of surface water into T1 and T2 aquifers is not warrant based on vertical profiles of ^{14}C next to the Torrens River. For example, wells 6d, 6c and 6b, located at just 50 m distance from the Torrens River and screened in the T1 aquifer at 111–117, 168–174, 212–218 mbg, respectively, have ^{14}C activities of 29.73, 4.25 and 3.62 pmC, respectively. Well 6a, at the same location but screened in the T2 aquifer at 245–251 mbg, has 2.59 pmC. If vertical recharge from the Torrens River would occur, higher ^{14}C activities would be expected, at least for the top part of the T1 aquifer.

The presence of NO_3^- in groundwater is originated by return flow from agricultural irrigation and/or human and animal waste either caused by septic tanks, sewage or exposed animal manure on farmland. In the Adelaide Plains relatively high concentrations of NO_3^- were found in the Q aquifer, occasional presence of nitrate in the T1 aquifer was found, and was undetectable or close to the detection limit in the T2 aquifer. Overall this suggests that recharge to T1 and T2 aquifers from the overlying Q aquifer is not a dominant process. Undetectable concentrations of NO_3^- in T1 and T2 aquifers could be also explained by ongoing denitrification processes as groundwater flows towards deeper layers, but denitrification primarily occurs in the absence of oxygen (Soares, 2000), and DO in Q and T1 aquifers was typically found to be 5–10 mg L^{-1}, concentrations that certainly can inhibit denitrification (Gómez et al., 2002), in which case nitrate would be likely to be found in deeper layers, but this is not the case.

Mass balance using Cl concentrations could potentially be used to estimate the contribution of Q and FRA aquifers into T1 and T2 aquifers. However, the similarity of Cl concentrations between Q and T2 aquifers (600–700 mg L^{-1}) in the Central and Southern Transects could provide misleading results from mass balance calculations. An analysis of pre-development (1940s) piezometric heads could potentially bring light to the direction of groundwater vertical flow. Unfortunately this type of data does not exist, and an analysis of post-development piezometric heads does not necessarily provide insight into sources of groundwater, because the groundwater system has been extensively pumped since 1940s. For example, an analysis (not shown) of historic (1980s) piezometric heads between ADE139 (T2 well) and ADE140 (T3 well) in the Central Adelaide Plains shows a positive difference of 2 m, resulting in a flow direction upwards from T3 into T2. This would suggest an additional potential source of Cl to the T2, other than from Q and FRA aquifers. Based on wells 1b (T2 aquifers) and 1a (FRA aquifer), the flow direction is upwards (from FRA to T2), but downwards (from T2 to FRA) based on wells 3b (T2 aquifer) and 3a (FRA aquifer).

Our results do not rule out the presence of vertical leakage from the Q aquifer into T1 and T2 aquifers (e.g. vertical downward flow from Q to T1 in wells 3e (Q aquifer) and 3d (T1 aquifer)), but overall our data (Cl and ^{14}C) suggest that the FRA aquifer is the primary contributor of groundwater into the Tertiary aquifers. This is indicated by the presence of old water near the top of the T2 aquifer in several wells in the Northern (e.g., PTA115, PTG079) and Central Adelaide Plains (e.g., 1b, ADE061), and the increase in age with distance from the Western MLR observed in all three transects. Cl concentrations are also higher in the Q than in the T1 and T2 aquifers, indicating that vertical leakage from the Q is not the main source of groundwater in the Tertiary aquifers.

Chloride deposition from precipitation in coastal areas is spatially variable and depends upon a number of factors such as distance to the coast, elevation, terrain slope and vegetation (Bresciani et al., 2014; Guan et al., 2010). Nonetheless, a Cl concentration in rainfall of 5 mg L^{-1} is a reasonable estimate for the Adelaide Plains (Guan et al., 2010; Harrington, 2002; Zulfic et al., 2003). With an average Cl concentration within the FRA aquifer in the MLR of 290 mg L^{-1}, and a range of rainfall between 400 and 1000 mm y^{-1} (characteristic values for the Plains and MLR), we estimate a groundwater recharge rate between 10 and 27 mm y^{-1}. Based on this approach, and assuming that all recharge in the MLR (20 km wide, 70 km long, recharge area 1400 km^2) flows across the faults to the plains, we calculate a recharge volume for the Tertiary aquifers between 1×10^7 m^3 y^{-1} and

2.4×10^7 m^3 y^{-1}. Alternatively, we can use the range of groundwater flow velocities estimated in the T2 aquifer in the Northern Transect (0.3–1.8 m y^{-1}) to obtain an independent estimate of the recharge volume. Assuming a combined constant T1 + T2 aquifer thickness of 150 m along the EBF and PF (representative length of 70 km), a volume between 0.3×10^7 and 2×10^7 m^3 y^{-1} would flow from the MLR through the EBF towards the Adelaide Plains. These estimates are in reasonable agreement with Georgiou et al. (2011), who estimated that the volume of groundwater withdrawn from T1 and T2 aquifers (agricultural, industrial and recreational purposes) to be in the order of 3×10^7 m^3 y^{-1}. Although this estimate is subject to significant uncertainty, it is noteworthy that it is similar to the estimated recharge volume flowing from the Western MLR. It is important to stress, however, that pumping volumes over the last few decades would have not yet affected the regional groundwater velocities determined from ^{14}C and ^{4}He calculations, as the total volume extracted is a small proportion of the aquifer volume.

6.2. Groundwater flow velocities

Mean helium accumulation rates for the Northern and Central Transects were used to estimate flow velocities in both the Northern and Central Transects west of the AF and PF faults, resulting in 0.3 and 0.15 m y^{-1}, respectively. A mean flow velocity of 0.8 m y^{-1} was estimated in the Northern Transect using ^{14}C. Helium data was calibrated using ^{14}C, thus different velocities are in principle not expected. We hypothesize that differences in ^{4}He and ^{14}C velocities are an artefact due to mean accumulation rates and velocities calculated from scattered data in the same transect.

Radiocarbon and helium flow velocities can be compared to hydraulic velocities, calculated using available K_H and n_e estimates. Using a hydraulic gradient of 1.6×10^{-3}, which corresponds to a 1959 potentiometric surface (Shepherd, 1971; see Fig. S1), hydraulic velocities in the T2 aquifer in the Northern Transect span between 0.9 and 3.5 m y^{-1}. In the Central and Southern Transects, where the K_H range in the T2 aquifer is smaller compared to the Northern Transect, hydraulic flow velocities range between 0.9 and 1.3 m y^{-1}. Overall hydraulic velocities are higher by approximately a factor between two and four. These hydraulic velocities are calculated using a 1959 hydraulic gradient, while pumping in the area started in the late 1940s and early 1950s. That means that pre-development hydraulic gradients are expected to be lower than 1.6×10^{-3}, thus resulting in lower velocities. For example, a lower hydraulic gradient by a factor of two would result in hydraulic velocities between 0.5 and 2.1 m y^{-1} in the Northern Transect, comparable to the radiometric range velocities of 0.3–1.8 m y^{-1}. The present hydraulic gradient in the T2 aquifer in the Northern Transect, 8.7×10^{-3}, is higher by a factor of five compared to 1959, while hydraulic gradients in the Central Transect, upgradient and downgradient of the PF, are 7×10^{-3} and 3×10^{-3}.

The rate of increase in helium concentration with distance in the Central Transect west of PF is higher than in the Northern Transect by a factor of four. This higher rate can be explained by a lower flow velocity in the Central Transect west of the PF. A lower flow velocity west of the PF in the T2 aquifer in the Central Transect may be partly due to the vertical displacement created by the PF that separates the Tertiary aquifers west and east of that fault.

6.3. Faults and water mixing

Some high $^{14}C_{corr}$ activities were measured at considerable depth close to the faults that separate the Western MLR from the Plains (MPA140- 88.5 pmC- and ADE138 – 70.5 pmC- in the Northern and Central Transects, respectively), suggesting a possible preferential pathway of relatively modern groundwater across the fault and onto the Plains. In the Central Transect, three wells in the FRA (5a, 5b and YAT134) are located close to the PF, a fault that caused an important displacement of Tertiary sediments. These wells have the highest concentrations of Cl (~5000–10,000 mg L^{-1}) and Br$^-$ (15–32 mg L^{-1}) measured in this study, and have among the most depleted ^{2}H signatures (−31‰). Additionally, groundwater sampled out of these three FRA wells is very old, as suggested by the $^{14}C_{corr}$ activities (1–2 pmC) and ^{4}He concentrations (10^{-6}–10^{-4} cm^3 STP g^{-1}). Overall, several lines of evidence suggest of an ongoing upwelling of old groundwater through faults, in some cases possibly related to old brines. Mixing of highly saline old fluids with fresher young waters has been previously reported (Di Sipio et al., 2006; Kaudse et al., 2016; Mayer et al., 2014; Williams et al., 2013). The fault system in the Adelaide Plains was responsible of an important vertical displacement of strata, and is related to several minor (magnitudes between 1.7 and 3.8) and majors earthquakes (magnitudes 5.5), in the last century (http://minerals.statedevelopment.sa.gov.au/home). This suggests that tectonically active faults (in the particular case of Adelaide most probably due to the stress caused by the Indo-Australian plate moving northwards), can play a role as preferential flow paths for the transport of old fluids rich in helium. Previous studies correlated the presence of deep helium with active faults and seismicity (Kulongoski et al., 2005; Newell et al., 2005; Wei et al., 2015).

Thus, faults may contribute to both upwelling of old saline "brine- related" fluids, but also infiltration of modern water near the recharge area. The direction of flow will be related to the vertical head gradient in the vicinity of the fault, although this is difficult to measure, and has likely been affected by recent pumping. Estimates of vertical velocities for these wells range between 0.01 and 0.4 m y^{-1}.

It is likely that some of the poor relationships observed between ^{4}He and $^{14}C_{corr}$ ages in the Adelaide Plains is due to mixing young with old groundwater in deeper parts of the aquifer. Upwelling of old groundwater through faults contributes to increase ^{4}He concentrations but does not significantly dilute ^{14}C.

7. Conclusions

Our study has shown the potential of environmental tracers to study flow velocities and residence time of complex multilayered, semi-confined and faulted aquifer systems. Groundwater flow velocities between 0.3 and 1.8 m y^{-1} were estimated using ^{14}C ages, resulting in basin recharge estimates between 0.3×10^7 and 2×10^7 m^3 y^{-1}. Faults were found to play a critical role mixing old and young water, highlighting the need to use several environmental tracers covering a wide range of residence times. For example, although radiocarbon and ^{4}He-estimated flow velocities were generally in good agreement, the range of ^{4}He accumulation rates confirmed slower flow velocities in some areas that could not be captured using ^{14}C. Carbon-14 has advantages over helium for measuring groundwater velocities, because apparent helium ages are greatly affected by small contributions of very old water. However, this particularity makes helium most sensitive to upward movement of old water through faults, and this was found to be useful in explaining some anomalies in chloride concentrations. Our study has also highlighted that highly complex groundwater systems require increased data density to accurately characterize the system. This is likely to prove a major impediment to detailed understanding of regional flow in complex hydrogeological systems.

Acknowledgements

Funding for this research was provided by the National Centre for Groundwater Research and Training, an Australian Government

initiative, supported by the Australian Research Council and the National Water Commission and, by the Goyder Institute for Water Research project "Assessment of Adelaide Plains Groundwater Resources". Thanks are owed to Lawrence Burk, Nicholas White, Stanley Smith, Chris Turnadge and Adrian Costar for their availability and assistance during sampling. Access and sampling of several wells could not have been possible without permission and co-operation of the councils of Marion, West Torrens and Mitcham, rangers of Cleland Conservation Park, personnel of the Holcim Australia – Montacute Quarry, the University of Adelaide Services (Hartley House), Assets and Technology Department of the Department of Environment, Water and Natural Resources in Adelaide, personnel of Saint Michaels College in Henley Beach, and numerous private land owners. Thanks are due to Mark Schoneweis for his help preparing some of the figures. Authors are grateful for comments provided by Dr. Lhoussaine Bouchaou and one anonymous reviewer. All data necessary to evaluate and build upon the work in this paper is available in the cited references and in the supplemental files.

Appendix A. Supplementary material

Supplementary data associated with this article can be found, in the online version, at http://dx.doi.org/10.1016/j.jhydrol.2016.12.036. These data include Google maps of the most important areas described in this article.

References

Andrews, J.N., Lee, D.J., 1979. Inert gases in groundwater from the Bunter Sandstone of England as indicators of age and palaeoclimatic trends. J. Hydrol. 41, 233–252. http://dx.doi.org/10.1016/0022-1694(79)90064-7.

Baird, D.J., 2010. Groundwater recharge and flow mechanisms in a perturbed, buried aquifer system: Northern Adelaide Plains, South Australia. School of Chemistry, Physics and Earth Sciences: 238.

Bense, V.F., Gleeson, T., Loveless, S.E., Bour, O., Scibek, J., 2013. Fault zone hydrogeology. Earth Sci. Rev. 127, 171–192. http://dx.doi.org/10.1016/j.earscirev.2013.09.008.

Bense, V.F., Person, M.A., 2006. Faults as conduit-barrier systems to fluid flow in siliciclastic sedimentary aquifers. Water Resour. Res. 42 (5), W05421. http://dx.doi.org/10.1029/2005WR004480.

Bense, V.F., Person, M.A., Chaudhary, K., You, Y., Cremer, N., Simon, S., 2008. Thermal anomalies indicate preferential flow along faults in unconsolidated sedimentary aquifers. Geophys. Res. Lett. 35 (24), L24406. http://dx.doi.org/10.1029/2008GL036017.

Beyerle, U., Aeschbach-Hertig, W., Hofer, M., Imboden, D.M., Baur, H., Kipfer, R., 1999. Infiltration of river water to a shallow aquifer investigated with $^{3}H/^{3}He$, noble gases and CFCs. J. Hydrol. 220, 169–185. http://dx.doi.org/10.1016/S0022-1694(99)00069-4.

Brennwald, M.S., Schmidt, M., Oser, J., Kipfer, R., 2016. A portable and autonomous mass spectrometric system for on-site environmental gas analysis. Environ. Sci. Technol. 50 (24), 13455–13463. http://dx.doi.org/10.1021/acs.est.6b03669.

Bresciani, E., Ordens, C.M., Werner, A.D., Batelaan, O., Guan, H., Post, V.E.A., 2014. Spatial variability of chloride deposition in a vegetated coastal area: implications for groundwater recharge estimation. J. Hydrol. 519, 1177–1191. http://dx.doi.org/10.1016/j.jhydrol.2014.08.050.

Cartwright, I., Morgenstern, U., 2012. Constraining groundwater recharge and the rate of geochemical processes using tritium and major ion geochemistry: Ovens Catchment, southeast Australia. J. Hydrol. 475 (137–149). http://dx.doi.org/10.1016/j.jhydrol.2012.09.037.

Castro, M.C., 2004. Helium sources in passive margin aquifers—new evidence for a significant mantle ^{3}He source in aquifers with unexpectedly low in situ $^{3}He/^{4}He$ production. Earth Planet. Sci. Lett. 222 (3–4), 897–913. http://dx.doi.org/10.1016/j.epsl.2004.03.031.

Castro, M.C., Goblet, P., 2005. Calculation of ground water ages—a comparative analysis. Ground Water 43 (3), 368–380. http://dx.doi.org/10.1111/j.1745-6584.2005.0046.x.

Clark, I., Fritz, P., 1997. Environmental Isotopes in Hydrogeology. CRC Press LLC, 331pp.

Cook, P.G., Bohlke, J.K., 2000. Determining timescales for groundwater flow and solute transport. In: Cook, P.G., Herczeg, A. (Eds.), Environmental Tracers in Subsurface Hydrology. Kluwer, Boston, pp. 1–30.

Cook, P.G., Love, A.J., Robinson, N.I., Simmons, C.T., 2005. Ground water ages in fractured rock aquifers. J. Hydrol. 308, 284–301. http://dx.doi.org/10.1016/j.jhydrol.2004.11.005.

Cook, P.G., Robinson, N.I., 2002. Estimating groundwater recharge in fractured rock from environmental 3H and 36Cl, Clare Valley, South Australia. Water Resour. Res., 38(8): 11-1–11-13. http://dx.doi.org/10.1029/2001WR000772.

Cook, P.G., Simmons, C.T., 2013. Using environmental tracers to constrain flow parameters in fractured rock aquifers; Clare Valley, South Australia. Dynamics of Fluids in Fractured Rock. Am. Geophys. Union, pp. 337–347.

Cranswick, R.H., Cook, P.G., 2015. Appendix D. Groundwater – surface water exhange. In: Assessment of Adelaide Plains Groundwater Resources: Appendices Part I – Field and Desktop Investigations, Goyder Institute for Water Research Technical Report Series No. 15/32, Adelaide, South Australia, 73–103 pp.

Crosbie, R.S., Morrow, D., Cresswell, R.G., Leaney, F.W., Lamontagne, S., Lefournour, M., 2012. New Insights Into the Chemical and Isotopic Composition of Rainfall Across Australia. CSIRO Water for a Healthy Country Flagship, Australia, p. 86.

DFW, 2011. Northern Adelaide Plains PWA. Groundwater level and salinity status report 2009–2010, Department for water, Government of South Australia.

Di Sipio, E., Galgaro, A., Zuppi, G.M., 2006. New geophysical knowledge of groundwater systems in Venice estuarine environment. Estuar. Coast. Shelf Sci. 66 (1–2), 6–12. http://dx.doi.org/10.1016/j.ecss.2005.07.015.

Dighton, J.C., Herczeg, A.L., Leaney, F.W., Lennard, R.P., Love, A.J., Gerges, N.Z., 1994. Stable isotope and radiocarbon data for groundwaters from the Adelaide metropolitan area. Report No. 56, Centre for Groundwater Studies.

Doyle, J.M., Gleeson, T., Manning, A.H., Mayer, K.U., 2015. Using noble gas tracers to constrain a groundwater flow model with recharge elevations: a novel approach for mountainous terrain. Water Resour. Res. 51 (10), 8094–8113. http://dx.doi.org/10.1002/2015WR017274.

Drimmie, R.J., Aravena, R., Wassenaar, L.I., Fritz, P., James Hendry, M., Hut, G., 1991. Radiocarbon and stable isotopes in water and dissolved constituents, Milk River aquifer, Alberta, Canada. Appl. Geochem. 6 (4), 381–392. http://dx.doi.org/10.1016/0883-2927(91)90038-Q.

Gardner, P., Solomon, D.K., 2009. An advanced passive diffusion sampler for the determination of dissolved gas concentrations. Water Resour. Res. 45 (6), W06423. http://dx.doi.org/10.1029/2008wr007399.

Gat, J.R., 1996. Oxygen and hydrogen isotopes in the hydrologic cycle. Annu. Rev. Earth Planet. Sci. 24 (1), 225–262. http://dx.doi.org/10.1146/annurev.earth.24.1.225.

Georgiou, J., Stadter, M., Purczel, C., 2011. Adelaide Plains groundwater flow and solute transport model, RPS Aquaterra, 162 pp.

Gerges, N.Z., 1999. The geology and hydrogeology of the Adelaide metropolitan area. School Earth Sci.

Gómez, M.A., Hontoria, E., González-López, J., 2002. Effect of dissolved oxygen concentration on nitrate removal from groundwater using a denitrifying submerged filter. J. Hazard. Mat. 90 (3), 267–278. http://dx.doi.org/10.1016/S0304-3894(01)00353-3.

Green, G., Watt, E., Alcoe, D., Costar, A., Mortimer, L., 2010. Groundwater Flow Across Regional Scale Faults, Science. Monitoring and Information Division, Department of Water, Land and Biodiversity Conservation, Adelaide, South Australia, p. 124.

Guan, H., Love, A.J., Simmons, C.T., Makhnin, O., Kayaalp, A.S., 2010. Factors influencing chloride deposition in a coastal hilly area and application to chloride deposition mapping. Hydrol. Earth Syst. Sci. 14 (5), 801–813. http://dx.doi.org/10.5194/hess-14-801-2010.

Guan, H., Zhang, X., Skrzypek, G., Sun, Z., Xu, X., 2013. Deuterium excess variations of rainfall events in a coastal area of South Australia and its relationship with synoptic weather systems and atmospheric moisture sources. J. Geophys. Res.: Atmospheres, 118(2):1123–1138. http://dx.doi.org/10.1002/jgrd.50137.

Harrington, G.A., 2002. Recharge mechanisms to Quaternary sand aquifers in the Willunga Basin, South Australia. DWLBC 2002/016, Department of Water, Land and Biodiversity Conservation, Adelaide, South Australia, 37pp.

Harrington, N., Cook, P.G., 2014. Groundwater in Australia. National Centre for Groundwater Research and Training, Australia, p. 40.

Houben, G.J., Koeniger, P., Sültenfuß, J., 2014. Freshwater lenses as archive of climate, groundwater recharge, and hydrochemical evolution: insights from depth-specific water isotope analysis and age determination on the island of Langeoog, Germany. Water Resour. Res. 50 (10), 8227–8239. http://dx.doi.org/10.1002/2014WR015584.

Kalin, R.M., 2000. Radiocarbon dating of groundwater systems. In: Cook, P.G., Herczeg, A.L. (Eds.), Environmental Tracers in Subsurface Hydrology. Kluwer Academic Publishers, pp. 111–144.

Kaudse, T., Bani-Khalaf, R., Tuffaha, R., Freundt, F., Aeschbach-Hertig, W., 2016. Noble gases reveal the complex groundwater mixing pattern and origin of salinization in the Azraq Oasis, Jordan. Appl. Geochem. 66, 114–128. http://dx.doi.org/10.1016/j.apgeochem.2015.12.003.

Kulongoski, J.T., Hilton, D.R., Izbicki, J.A., 2003. Helium isotope studies in the Mojave Desert, California: implications for groundwater chronology and regional seismicity. Chem. Geol. 202, 95–113. http://dx.doi.org/10.1016/j.chemgeo.2003.07.002.

Kulongoski, J.T., Hilton, D.R., Izbicki, J.A., 2005. Source and movement of helium in the eastern Morongo groundwater Basin: the influence of regional tectonics on crustal and mantle helium fluxes. Geochim. Cosmochim. Acta 69 (15), 3857–3872. http://dx.doi.org/10.1016/j.gca.2005.03.001.

Lehmann, B.E., Love, A., Purtschert, R., Collon, P., Loosli, H.H., Kutschera, W., Beyerle, U., Aeschbach-Hertig, W., Kipfer, R., Frape, S.K., Herczeg, A., Moran, J., Tolstikhin, I.N., Gröning, M., 2003. A comparison of groundwater dating with ^{81}Kr, ^{36}Cl and ^{4}He in four wells of the Great Artesian Basin, Australia. Earth Planet. Sci. Lett. 211, 237–250. http://dx.doi.org/10.1016/S0012-821X(03)00206-1.

Liu, J., Fu, G., Song, X., Charles, S.P., Zhang, Y., Han, D., Wang, S., 2010. Stable isotopic compositions in Australian precipitation. J. Geophys. Res.: Atmospheres, 115 (D23): D23307. http://dx.doi.org/10.1029/2010JD014403.

Mächler, L., Brennwald, M.S., Kipfer, R., 2012. Membrane inlet mass spectrometer for the quasi-continuous on-site analysis of dissolved gases in groundwater. Environ. Sci. Technol. 46 (15), 8288–8296. http://dx.doi.org/10.1021/es3004409.

Mächler, L., Brennwald, M.S., Tyroller, L., Livingstone, D.M., Kipfer, R., 2014. Conquering the outdoors with on-site mass spectrometry. CHIMIA Int. J. Chem. 68 (3), 155–159. http://dx.doi.org/10.2533/chimia.2014.155.

Mächler, L., Peter, S., Brennwald, M.S., Kipfer, R., 2013. Excess air formation as a mechanism for delivering oxygen to groundwater. Water Resour. Res. 49 (10), 6847–6856. http://dx.doi.org/10.1002/wrcr.20547.

Mahlknecht, J., Schneider, J., Merkel, B., Navarro de León, I., Bernasconi, S., 2004. Groundwater recharge in a sedimentary basin in semi-arid Mexico. Hydrogeol. J. 12 (5), 511–530. http://dx.doi.org/10.1007/s10040-004-0332-6.

Manning, A.H., Solomon, D.K., 2005. An integrated environmental tracer approach to characterizing groundwater circulation in a mountain block. Water Resour. Res. 41 (12), W12412. http://dx.doi.org/10.1029/2005WR004178.

Mayer, A., May, W., Lukkarila, C., Diehl, J., 2007. Estimation of fault-zone conductance by calibration of a regional groundwater flow model: Desert Hot Springs, California. Hydrogeol. J. 15 (6), 1093–1106. http://dx.doi.org/10.1007/s10040-007-0158-0.

Mayer, A., Sültenfuß, J., Travi, Y., Rebeix, R., Purtschert, R., Claude, C., Le Gal La. Salle, C., Miche, H., Conchetto, E., 2014. A multi-tracer study of groundwater origin and transit-time in the aquifers of the Venice region (Italy). Appl. Geochem. 50, 177–198. http://dx.doi.org/10.1016/j.apgeochem.2013.10.009.

Mays, L.W., 2013. Groundwater resources sustainability: past, present, and future. Water Resour. Manage 27 (13), 4409–4424. http://dx.doi.org/10.1007/s11269-013-0436-7.

McMahon, P.B., Böhlke, J.K., Christenson, S.C., 2004. Geochemistry, radiocarbon ages, and paleorecharge conditions along a transect in the central High Plains aquifer, southwestern Kansas, USA. Appl. Geochem. 19 (11), 1655–1686. http://dx.doi.org/10.1016/j.apgeochem.2004.05.003.

Medeiros, W.E., do Nascimento, A.F., Alves da Silva, F.C., Destro, N., Demétrio, J.G.A., 2010. Evidence of hydraulic connectivity across deformation bands from field pumping tests: two examples from Tucano Basin, NE Brazil. J. Struct. Geol. 32 (11), 1783–1791. http://dx.doi.org/10.1016/j.jsg.2009.08.019.

Newell, D.F., Crossey, L.J., Karlstrom, K.E., Fischer, T.P., Hilton, D.R., 2005. Continental-scale links between the mantle and groundwater systems of the western United States: evidence from travertine springs and regional He isotope data. GSA Today 15 (12), 4–10. http://dx.doi.org/10.1130/1052-5173(2005)015<4:CSLBTM>2.0.CO;2.

Pearson, F.J., Hanshaw, B.B., 1970. Sources of Dissolved Carbonate Species in Groundwater and Their Effects on Carbon-14 Dating. Proc. of the IAEA Isotope Hydrology, Vienna, Austria, pp. 271–286.

Plummer, L.N., Eggleston, J.R., Andreasen, D.C., Raffensperger, J.P., Hunt, A.G., Casile, G.C., 2012. Old groundwater in parts of the upper Patapsco aquifer, Atlantic Coastal Plain, Maryland, USA: evidence from radiocarbon, chlorine-36 and helium-4. Hydrogeol. J. 20 (7), 1269–1294. http://dx.doi.org/10.1007/s10040-012-0871-1.

Poole, J.C., McNeill, G.W., Langman, S.R., Dennis, F., 1997. Analysis of noble gases in water using a quadrupole mass spectrometer in static mode. Appl. Geochem. 12 (6), 707–714. http://dx.doi.org/10.1016/S0883-2927(97)00043-7.

Price, R.M., Top, Z., Happell, J.D., Swart, P.K., 2003. Use of tritium and helium to define groundwater flow conditions in Everglades National Park. Water Resour. Res. 39 (9), 1267. http://dx.doi.org/10.1029/2002WR001929.

Raiber, M., Webb, J.A., Cendón, D.I., White, P.A., Jacobsen, G.E., 2015. Environmental isotopes meet 3D geological modelling: conceptualising recharge and structurally-controlled aquifer connectivity in the basalt plains of south-western Victoria, Australia. J. Hydrol. 527, 262–280. http://dx.doi.org/10.1016/j.jhydrol.2015.04.053.

Roques, C., Aquilina, L., Bour, O., Maréchal, J.-C., Dewandel, B., Pauwels, H., Labasque, T., Vergnaud-Ayraud, V., Hochreutener, R., 2014. Groundwater sources and geochemical processes in a crystalline fault aquifer. J. Hydrol., 519, Part D: 3110–3128. http://dx.doi.org/10.1016/j.jhydrol.2014.10.052.

Shepherd, R.G., 1971. The hydrogeology of the Northern Adelaide Plains Basin. Mineral Resources Rev., South Australia 134, 52–61.

Soares, M.I.M., 2000. Biological denitrification of groundwater. Water Air Soil Poll. 123 (1), 183–193. http://dx.doi.org/10.1023/a:1005242600186.

Solomon, D.K., 2000. ^{4}He in groundwater. In: Cook, P.G., Herczeg, A. (Eds.), Environmental Tracers in Subsurface Hydrology. Kluwer Academic Publishers, pp. 425–439.

Stoessell, R.K., Prochaska, L., 2005. Chemical evidence for migration of deep formation fluids into shallow aquifers in South Louisiana. Gulf Coast Assoc. Geol. Soc. Trans., 55: 794–808.

Stuiver, M., Polach, H.A., 1977. Discussion. Reporting of 14C data. Radiocarbon, 19 (3): 355–363.

Torgersen, T., Clarke, W.B., 1985. Helium accumulation in groundwater, I: an evaluation of sources and the continental flux of crustal ^{4}He in the Great Artesian Basin, Australia. Geochim. Cosmochim. Acta 49 (5), 1211–1218. http://dx.doi.org/10.1016/0016-7037(85)90011-0.

Torgersen, T., Habermehl, M.A., Phillips, F.M., Elmore, D., Kubik, P., Jones, G.B., Hemmick, T., Gove, H.E., 1991. Chlorine 36 Dating of Very Old Groundwater: 3. Further Studies in the Great Artesian Basin, Australia. Water Resour. Res. 27 (12), 3201–3213. http://dx.doi.org/10.1029/91WR02078.

Torgersen, T., Ivey, G.N., 1985. Helium accumulation in groundwater. II: A model for the accumulation of the crustal ^{4}He degassing flux. Geochim. Cosmochim. Acta 49 (11), 2445–2452. http://dx.doi.org/10.1016/0016-7037(85)90244-3.

Vairavamoorthy, K., Gorantiwar, S.D., Pathirana, A., 2008. Managing urban water supplies in developing countries – Climate change and water scarcity scenarios. Phys. Chem. Earth, Parts A/B/C, 33(5): 330–339. http://dx.doi.org/10.1016/j.pce.2008.02.008.

Varsányi, I., Matray, J.-M., Kovács, L.Ó., 1997. Geochemistry of formation waters in the Pannonian Basin (southeast Hungary). Chem. Geol. 140, 89–106. http://dx.doi.org/10.1016/S0009-2541(97)00045-4.

Vogel, J.C., 1970. Carbon-14 Dating of Groundwater. Proc. of the Isotope Hydrology, Vienna, Austria, pp. 225–240.

Wei, W., Aeschbach-Hertig, W., Chen, Z., 2015. Identification of He sources and estimation of He ages in groundwater of the North China Plain. Appl. Geochem. 63, 182–189. http://dx.doi.org/10.1016/j.apgeochem.2015.08.010.

Weiss, R.F., 1970. Helium isotope effect in solution in water and seawater. Science 168 (3928), 247–248. http://dx.doi.org/10.1126/science.168.3928.247.

Williams, A.J., Crossey, L.J., Karlstrom, K.E., Newell, D., Person, M., Woolsey, E., 2013. Hydrogeochemistry of the Middle Rio Grande aquifer system—fluid mixing and salinization of the Rio Grande due to fault inputs. Chem. Geol. 351, 281–298. http://dx.doi.org/10.1016/j.chemgeo.2013.05.029.

Zulfic, D., Barnett, S.R., van den Akker, J., 2003. Mount Lofty Ranges Groundwater Assessment, Upper Onkaparinga Catchment. DWLBC 2002/29, Deparment of Water, Land and Biodiversity Conservation, Adelaide, South Australia, 53pp.

Zulfic, H., Osei-Bonsu, K., Barnett, S.R., 2008a. Adelaide metropolitan area groundwater modelling project. Volume 1 – Review of hydrogeology. 2008/5, Department of Water, Land and Biodiversity Conservation (DWLBC), Adelaide, South Australia.

Zulfic, H., Osei-Bonsu, K., Barnett, S.R., 2008b. Adelaide metropolitan area groundwater modelling project. Volume 2 – Numerical model development prediction run. 2008/5, Department of Water, Land and Biodiversity Conservation (DWLBC), Adelaide, South Australia.

http://minerals.statedevelopment.sa.gov.au/home (Last accessed on 12.10.2016).

http://wds.amlr.waterdata.com.au/Amlr.aspx (Last accessed on 12.10.2016).